Mismatch between coccolithophore-based estimates of particulate inorganic carbon (PIC) concentration and satellite-derived PIC concentration in the Pacific Southern Ocean

Mariem Saavedra-Pellitero[1], Karl-Heinz Baumann[2], Nuria Bachiller-Jareno[1-3], Harold Lovell[1], Nele Manon Vollmar[2-4], Elisa Malinverno[5]

[1]School of the Environment and Life Sciences, University of Portsmouth, Portsmouth, PO1 3QL, United Kingdom
[2]Department of Geosciences, University of Bremen, 28334, Bremen, Germany
[3]Department of Computer Science, University of Exeter, Exeter, Streatham Campus, Rennes Drive, Exeter EX4 4RN
[4]NORCE Norwegian Research Centre AS, NORCE Climate & Environment, 5007, Bergen, Norway and Bjerknes Centre for Climate Research, Bergen, Norway
[5]Department of Geological Sciences and Geotechnologies, Milano-Bicocca University, 20126, Milan, Italy

Correspondence to: Mariem Saavedra-Pellitero (mariem.saavedra-pellitero@port.ac.uk)

Abstract

Coccolithophores are the main type of calcifying phytoplankton in the Southern Ocean (SO) and are key organisms in the production of particulate inorganic carbon (PIC). However, in situ studies of coccolithophores and in particular of their importance for the input of PIC in the SO are sparse in space and time due to its inaccessibility. An alternative tool for monitoring PIC is the use of optical remote sensing, as coccolithophores account for most of the optical PIC backscattering in the sea. The aim of the present study is to provide coccolithophore-based estimates of PIC derived from Scanning Electron Microscope coccolith morphometric analyses and MODIS-Aqua Level 2 and Level 3 PIC concentration values along two latitudinal transects from New Zealand to Antarctica and across the Drake Passage. In general, the coccolith-estimated PIC and satellite-derived PIC datasets show comparable trends in the Subantarctic and Polar Front Zones of both transects, with coccolith-derived PIC values being generally lower than PIC-satellite values. According to the coccolithophorid data, *Emiliania huxleyi* type A, type A overcalcified, and other taxa (e.g. *Calcidiscus leptoporus*), only contribute to coccolithophore PIC in the northernmost sampling locations, whereas *E. huxleyi* morphogroup B substantially contributes to the PIC content south of the Subantarctic Front in both transects. High satellite-derived PIC concentrations south of the Polar Front are not apparent in the coccolith-based PIC data. We suggest that the high reflectance signal at the Antarctic Zone may instead relate to the presence of small biogenic opal particles (e.g. diatoms, silicoflagellates and/or small siliceous plankton) or other unknown highly reflective particles (such as *Phaeocystis* aggregations). Our results highlight the challenges presented by the

lack of reliable satellite data in some parts of the SO as well as the importance of in situ measurements and methodological accuracy when estimating PIC values.

1 Introduction

Coccolithophores are a major component of calcifying phytoplankton communities in the Southern Ocean (SO) (e.g. Saavedra-Pellitero et al., 2014; Saavedra-Pellitero et al., 2019; Malinverno et al., 2015; Charalampopoulou et al., 2016; Rigual Hernández et al., 2020a) and play an important and complex role in the carbon cycle through the production of particulate inorganic carbon (PIC) and particulate organic carbon (POC) (e.g. Rost and Riebesell, 2004; Salter et al., 2014). These haptophyte algae produce an external covering (coccosphere) of interlocking calcite platelets (coccoliths). Coccolith calcification decreases the alkalinity of surface waters, thereby reducing the uptake of CO_2 from the atmosphere into the surface ocean and thus acting in opposition to photosynthetic carbon fixation (Rost and Riebesell, 2004). Furthermore, coccolithophores influence the export of PIC and POC to the deep ocean through the ballasting effects of their coccoliths into the deep sea (e.g. Klaas and Archer, 2002). Previous work has suggested that calcification during blooms of the coccolithophore *Emiliania huxleyi*, aka *Gephyrocapsa huxleyi* (Bendif et al., 2023), might alter the air-sea flux of CO_2 (e.g. Harlay et al., 2010; Shutler et al., 2013), although to date, the impact of this has mostly only been explored on a limited regional basis (e.g. Holligan et al., 1993; Robertson et al., 1994; Balch et al., 2016).

Since the early days of satellite-based color measurements of the oceans, large coccolithophore blooms have been visible as highly reflective regions in satellite images (e.g. Holligan et al., 1983). Coccolithophores, and their detached coccoliths, are strongly optically active in the entire visible spectrum (400-700 nm) and notably affect the optical budget of the surface ocean; they can thus be seen from space using satellite remote sensing (Smyth et al., 2002; Tyrrell and Taylor, 1996). Coccolithophores are responsible for most of the optical PIC backscatter in the ocean; the other, larger PIC particles associated with foraminifera and pteropods provide negligible backscatter per unit mass and therefore have minimal optical impact (Balch et al., 1996). In general, detached coccoliths account for 10-20% of the total light backscattered from the sea under non-bloom conditions, whereas under bloom conditions it can be more than 90% (Balch et al., 1991; Balch et al., 1999). Gordon et al. (2001) and Balch et al. (2005) developed algorithms to estimate the PIC concentration in the surface layer of the water column from the radiance emanating from the water. The relationship between inherent optical properties and the resultant light fields is well understood (e.g. Mitchell et al., 2017). The difficulty lies in understanding the combined effects of different in-water constituents on the inherent optical properties, and ultimately, the underwater light fields. While there have been many advances in this area (e.g. Babin et al., 2003a; Babin et al., 2003b; Devred et al., 2006), there will always be some uncertainty in calculating these relationships. For example, it has been shown that satellite ocean-color-based PIC estimates did not match

(ship-based) in situ observations and that satellite-derived PIC can be overestimated in Antarctic waters (e.g. Holligan et al., 2010; Trull et al., 2018). One potential source of error is that aquamarine waters characterized by high reflectance of light can also be caused by suspended sediment and even opal particles, such as fragments of diatom frustules (e.g. Broerse et al., 2003).

The band of high reflectance and elevated PIC waters observed in the SO between 30°- 60° S during Austral summer, known as "the Great Calcite Belt", has been linked to a region of increased seasonal abundance of coccolithophores (Balch et al., 2011; Balch et al., 2016). Comparisons of in situ and remote sensing measurements of PIC have been undertaken in different sectors of the SO (mostly Atlantic and Indian) for coccolithophore bloom conditions (e.g. Holligan et al., 2010; Poulton et al., 2011; Balch et al., 2014; Balch et al., 2016; Oliver et al., 2023). However, this type of comparison is very limited in specific areas of the globe (such as the vast Pacific sector of the SO) and also in non-bloom coccolithophore conditions (e.g. Oliver et al., 2023). This is partially due to the fact that available coccolithophore measurements are sparse in space and time in the SO. Many of the subpolar studies focus on coccospheres, whilst there are scarce data on free coccoliths (Mohan et al., 2008).

Recent concerns about climate change have motivated the scientific community to focus on *E. huxleyi* as a target cosmopolitan species and in particular to differentiate it into different morphotypes (e.g., Young et al., 2003), which are included into two main morphogroups, A and B (Young et al., 2023). The high-latitude distribution of *E. huxleyi* has undergone a recent poleward expansion in both the northern (Rivero-Calle et al., 2015) and southern hemisphere (Cubillos et al., 2007; Winter et al., 2014). The sub-Antarctic realm is characterized by more calcified coccoliths north of the Subantarctic Front to more weakly calcified placoliths polewards (Cubillos et al., 2007). Significant zonal differences are shown in the relationship between coccolithophore data and Antarctic Circumpolar Current (ACC) frontal positions across the different sectors of the SO (e.g. Saavedra-Pellitero et al., 2014), but no strong evidence for recent expansion on a circumpolar scale has been identified (Malinverno et al., 2015). Several estimates of coccolith-PIC exist, e.g. estimation of coccolith mass from coccolith volume calculated from coccolith size (Young and Ziveri, 2000; Beuvier et al., 2019), using polarizing light microscopy (Beaufort, 2005; Bollmann, 2014; Fuertes et al., 2014) or the Coulter multisizer (i.e. electric field disturbance; Valença et al., 2024).

Here, we focus on the contribution of *E. huxleyi* and other coccolithophore taxa to sea surface PIC along two latitudinal transects across the ACC fronts: a New Zealand transect (sampled during December 2004-January 2005) and a Drake Passage transect (sampled during February-March 2016). Coccosphere concentrations in the New Zealand transect were below 1.4×10^5 cells/L and in the Drake Passage transect were below 1.5×10^5 cells/L (Malinverno et al., 2015; Saavedra-Pellitero et al., 2019), corresponding to non-bloom to moderate bloom conditions (Poulton et al., 2011). Our aims are: (1) to evaluate the contribution of different coccolithophore taxa and *E. huxleyi* morphotypes to coccolith-morphometric-based PIC estimates, and (2) to compare coccolith-derived PIC values with satellite-derived PIC values in the Pacific SO.

2 Study area: oceanographic setting and phytoplanktonic communities

The SO is a high-nutrient, low-chlorophyll area in the Southern Hemisphere (e.g. de Baar et al., 1995) that connects all the main oceans through the strong and eastward flowing ACC. In the SO, there are a number of oceanographic fronts characterized by increased horizontal transport and rapid changes in water properties (Orsi et al., 1995; Klinck and Nowlin, 2001). The ACC is bounded by the Subtropical Front (STF) in the north, which separates it from the warmer and saltier waters of the subtropics, and its southern edge is marked by the Southern Boundary, which separates it from subpolar cold, silicate-rich waters (Orsi et al., 1995). The ACC flow is mostly driven by the westerly winds. The position of the fronts varies seasonally as well as spatially, being controlled by steep topographic features, such as oceanic plateaus or ridges (Gordon et al., 1978). South of the STF, the Subantarctic Front (SAF) separates the Subantarctic Zone (SAZ) and the Polar Frontal Zone (PFZ) (Fig. 1). The location of the SAF is indicated by a strong thermal gradient and by the rapid northwards sinking of a salinity (S) minimum associated with the Antarctic Intermediate Water, from the surface in the PFZ (S<34) to depths greater than 300 m in the SAZ (S<34.20) (Orsi et al., 1995; Whitworth, 1980). South of the SAF, the prominent Polar Front (PF) separates the PFZ and the Antarctic Zone (AZ). The PF represents the northernmost extent of the 2°C isotherm at 200 m depth and corresponds to a 2°C gradient in sea surface temperature (Orsi et al., 1995). The Southern ACC Front is characterized by temperatures below 0°C at the minimum temperature in the sub-surface (<150 m) and above 1.8°C at the maximum temperature at depths >500 m (Orsi et al., 1995). A more detailed description of the property indicators at each SO front can be found in Orsi et al. (1995).

Coccolithophores are important components of some of the SO phytoplankton communities, especially in the SAZ, where they reach relatively high numbers and diversity (e.g. Gravalosa et al., 2008; Saavedra-Pellitero et al., 2014; Malinverno et al., 2015; Charalampopoulou et al., 2016; Saavedra-Pellitero et al., 2019; Rigual Hernández et al., 2020a). South of the PF, diatoms and other siliceous microfossils dominate (e.g. Saavedra-Pellitero et al., 2014; Malinverno et al., 2016; Cárdenas et al., 2018). The coccolithophore abundance and diversity in the Drake Passage drastically drop from north to south, with the oceanographic fronts appearing to act as ecological boundaries (Saavedra-Pellitero et al., 2019), whereas the total coccolithophore abundance is highest in the PFZ south of New Zealand (Malinverno et al., 2015). Similar marked shifts in coccolithophore numbers, community composition, and diversity at the SAF and PF were also previously noted in other sectors of the SO (e.g. Mohan et al., 2008; Gravalosa et al., 2008; Holligan et al., 2010; Saavedra-Pellitero et al., 2014; Balch et al., 2016; Charalampopoulou et al., 2016) and are in accordance with previous observations in both transects (Malinverno et al., 2015; Saavedra-Pellitero et al., 2019). In particular, the PF (Drake Passage) and the Southern ACC Front (New Zealand transect) are natural barriers marked by a clear drop in the number of *E. huxleyi*, which often is the only species found in the PFZ and almost always occurs as B morphogroup (types B/C and O). Furthermore, a general southwards decreasing trend in *E. huxleyi* mass, linked to a latitudinal trend from more calcified *E. huxleyi* (A morphogroup) to weakly calcified morphotypes (B morphogroup), was already recorded across the Drake Passage (Saavedra-Pellitero et al., 2019).

3 Materials and methods

3.1 Sampling considerations and morphometrics

3.1.1 The New Zealand transect

Forty-two surface water samples were collected from the ship's pump of the *R/V Italica* (at ca. 3 m water depth) from 46.81°S to 69.37°S during the XX Italian Expedition from New Zealand to Antarctica from 31st December 2004 to 6th January 2005 (Fig. 1, Table 1). Details on sample locations, sampling volume, coccolithophore and coccolith counts can be found in Malinverno et al. (2015).

We selected a total of 13 water samples for Scanning Electron Microscope (SEM Tescan Vega at the University of Milano-Bicocca) morphometric analyses of *E. huxleyi* covering the various biogeographic zones across the ACC (Fig. 1). For each sample, 30-50 images of *E. huxleyi* free coccoliths and coccospheres were collected as encountered during filter scanning (377 images in total, Table 1S in Supplementary Material). Distal shield length and width, tube thickness, and number and thickness of distal shield elements were manually measured in micrometers (µm) based on the scalebar of the SEM images using the ImageJ software (Schneider et al., 2012) (Fig. 2).

3.1.2 The Drake Passage transect

Nineteen water samples were collected on a transect at the western end of the Drake Passage from 55.44°S to 61.75°S during the *Polarstern* Expedition PS97 from 24th February 2016 to 5th March 2016 (Fig. 1, Table 1). These selected plankton samples were obtained using a rosette sampler with 24×12 L Niskin bottles (Ocean Test Equipment Inc.) attached to a CTD Seabird SBE911plus device (Lamy, 2016). The bottles were fired by a SBE32 carousel and just the shallowest samples, from 5, 10 and 20 m water depth, were considered in this work. Details on sample locations, sampling volume, coccolithophore assemblages and coccospheres/L can be found in Saavedra-Pellitero et al. (2019).

A total of 203 images of *E. huxleyi* coccospheres were taken from the samples in the Drake Passage while scanning the filters within another SEM (Zeiss DSM 940A at the Geosciences Faculty, University of Bremen; Table 2S in Supplementary Material). Coccoliths were measured using the Coccobiom2 macro (Young, 2015) in the software program Fiji, an image processing package based on ImageJ (Schindelin et al., 2012). Measurements were made in µm, based on the scale bar of the SEM images. Note that the images were scaled to 100% with a Coccobiom2 SEM calibration of 1.09 and the specific magnification.

3.2 Coccolithophore taxonomical considerations

Emiliania huxleyi specimens were classified following Young et al. (2003) and Young et al. (2023) during the SEM morphometric analyses. Initially, six different morphotypes were distinguished in the study area, belonging to morphogroups A and B (for further details, see Table 2). These are *E. huxleyi* type A, type A overcalcified, type B, type B/C, type C and type O. Specific taxonomical considerations regarding the rest of the coccolithophore taxa can be found in Malinverno et al. (2015) and Saavedra-Pellitero et al. (2019).

3.3 Coccolithophore PIC estimates

Species-specific coccolith-PIC (in pmol) was estimated following the volume calculation of Young and Ziveri (2000)

$$PIC = (2.7 \times Ks \times L^3) \div 100 \qquad \text{[equation 1]}$$

where:

2.7 = density of calcite (pg μm^{-3});

Ks = species-specific shape factors, as provided by Young and Ziveri (2000) and modified for *E. huxleyi* according to the degree of calcification obtained for each morphotype as compiled by Vollmar et al. (2022) (further details in Table 3);

L = coccolith mean length from measurements (µm) in the case of *E. huxleyi*. For minor species, we considered the averaged coccolith length provided by Young and Ziveri (2000);

100 = molecular weight of calcite (g mol^{-1}).

Measurements of the distal shield diameters of *Calcidiscus leptoporus*, the secondmost abundant species that is significantly larger and much more massive than *E. huxleyi*, were made on different samples offshore of New Zealand, corresponding to the highest abundances of this taxa (Table 3 and Table 3S in Supplementary Material). The importance of making size measurements on the communities analyzed for the determination of species-dependent coccolith PIC, rather than using size measurements from the scientific literature, has been clearly emphasized (Baumann, 2004). The coccolith-PIC contribution for each sample was calculated by applying the obtained species-specific calcite quota to the abundances of species and morphotype (i.e., coccospheres/L) from Malinverno et al. (2015) and Saavedra-Pellitero et al. (2019) (Tables 1 and 3). In the New Zealand transect, the single or double coccolith layers were considered in the estimates (Table 1S in Supplementary Material), while in the Drake Passage transect, where this information was not available, an average was considered based on our own observations (Table 3 and Table 4S in Supplementary Material). Additionally, detached coccoliths/L were considered for the PIC estimates in the New Zealand transect (Malinverno et al., 2015). To estimate the number of coccoliths per coccosphere we counted the visible placoliths (half coccosphere) and multiplied by two (Table 4S).

We also calculated the relative tube width in *E. huxleyi* as a size-independent index to estimate the degree of calcification in this taxon following Young et al. (2014) (Fig. 2):

Relative tube width= (2×tube width)÷coccolith width [equation 2]

Note that because the relative tube width is a ratio, it is dimensionless, and it should be size-independent (Young et al., 2014).

3.4 Coccolith-estimated PIC errors

There are sources of errors and uncertainties linked to the approach chosen to estimate the coccolith PIC. To assess the precision of the measurements, two different coccoliths were measured 50 times each. The standard deviation (SD) for the coccolith length was 0.014 and 0.017 μm and the standard error 0.002 μm in both cases. Coccolith volume estimates are likely to contain errors around 40-50% according to Young and Ziveri (2000), so we assumed the largest potential error and added a 50% error bars to our plots. However, we note that measuring the actual size range in the sample can reduce this error to about 5-10% in length and 15-30% in volume, so we also added 15% error bars to our plots to show the minimum potential error.

3.5 Satellite-derived PIC and chlorophyll a data processing

To compare the coccolith-estimated PIC with satellite-derived values, PIC concentration (in mol m^{-3}) was obtained from the MODIS-Aqua Level (L) 2 and L3 products (NASA Goddard Space Flight Center, Ocean Ecology Laboratory, Ocean Biology Processing Group, 2022a). To encompass the broad range of PIC concentrations observed in the global ocean, a combination of two independent approaches is used to calculate the backscattering coefficient for PIC (the description of the algorithm can be found in NASA Ocean Biology Processing Group, 2023; for further details see also Balch and Mitchel, 2023). The Ocean Biology Processing Group validates MODIS-Aqua PIC retrievals against in situ measurements, which results in a mean bias of ± 0.31623 and a mean absolute error (MAE) of ± 3.91664 (both values calculated based on log10 transformation of the PIC values) (NASA Ocean Biology Processing Group, 2023). These metrics indicate the degree of accuracy and potential bias in the satellite-derived estimates compared to direct observations.

MODIS-Aqua L2 scenes encompassing both the sampling period and the geographical extent of each transect were downloaded from NASA's Ocean Color Level 1 and 2 browser (https://oceancolor.gsfc.nasa.gov/cgi/browse.pl). The downloaded MODIS L2 scenes corresponded to swaths covering at least 50% of the study area and included more than one daily scene. Table 4 summarizes the number of downloaded scenes as well as their time coverage. To obtain satellite-derived PIC concentration for comparison with coccolith-estimated PIC concentration at each sample location, the mean of a 5x5 window centered on the measurement location (Bailey and Werdell, 2006) was extracted from the downloaded scenes using the SNAP 9.0.0 pixel extraction tool (European Space Agency, 2022). This tool provides basic statistics, such as the number

of pixels (N) contributing to each mean value and the SD of these pixel values, allowing the homogeneity of the extraction point to be assessed. Pixels flagged with atmospheric correction failure (ATMFAIL) or very low water-leaving radiance (LOWLW) were excluded from the extraction. To ensure statistical confidence in the retrieved values, all PIC mean values resulting from the aggregation of 12 or fewer N within the 5x5 window were discarded (Bailey and Werdell, 2006). Duplicate daily mean PIC values (i.e. PIC values for a measuring location extracted from more than one scene captured on the same day) and their corresponding SD were then weighted according to their uncertainties (Bevington, 1969) to give more prominence to measurements with a lower SD, which are generally considered to be more reliable. Where the SD of daily mean values was equal to zero, these values were taken directly as the result as they are indicative of homogeneity.

Due to high cloud cover and other conditions that interfere with the detection of water-leaving radiances (NASA Ocean Biology Processing Group, 2023), daily PIC grids yielded a high number of missed observations, or gaps, which prevented us from acquiring daily satellite-derived PIC values of the sampling dates for most sample locations in both transects (Figs. 1S and 2S in Supplementary Material show the availability of MODIS-Aqua L2 PIC values across stations over the sampling period). This lack of cloud-free satellite images made it impossible to use a time window of 24 h to determine coincidence between coccolith-estimated PIC and satellite-derived PIC. Therefore, to increase the possibility of a ship-satellite match-up, we (1) extended the satellite period to seven days before and after sampling dates (see Table 4 for specific dates) and extracted the PIC for all sample locations, regardless of their sampling date. We deliberately chose that time range considering that *E. huxleyi* can double its numbers in two or three days without accounting for grazing by zooplankton (based on studies in the North Atlantic; Holligan et al., 1993), ensuring no drastic changes from non-coccolithophore bloom to bloom conditions. We then generated a mean PIC value for each location by aggregating the available daily means over the full period to explore the latitudinal variation of this variable. We also, independently, (2) obtained monthly (Figs. 3S and 4S in Supplementary Material) and 8-daily (hereafter referred to as weekly) satellite-derived PIC concentrations (mol m^{-3}) from the MODIS-Aqua L3 product (NASA Goddard Space Flight Center, Ocean Ecology Laboratory, Ocean Biology Processing Group, 2022b). This allowed us to have additional satellite-derived PIC values to compare to the coccolith-estimated PIC in the study area. Images encompassing both the sampling period and the geographical extent of each transect were acquired from NASA's Ocean Color Level 3 & 4 Browser (https://oceancolor.gsfc.nasa.gov/l3/) as 4 km cell size gridded files in NetCDF file format. Table 4 summarizes the number of downloaded scenes as well as their temporal coverage. The L3 extracted values corresponded to the PIC concentration of the grid cell enclosing the sample location. As per L2 data extraction, PIC concentrations for all sample locations were acquired from all available monthly and weekly scenes. MODIS-Aqua L2 chlorophyll a concentration in mg m^{-3} were also extracted and processed as an indicator of the presence of diatoms and other phytoplanktonic groups. The algorithm used to calculate chlorophyll a is documented by Werdell et al. (2023).

4 Results

4.1 Morphometries and mass estimates of *Emiliania huxleyi*

Emiliania huxleyi is the dominant species in the coccolithophore assemblage of the Pacific SO and it consist of different morphotypes that show a different and partly overlapping distribution along both latitudinal transects (Malinverno et al., 2015; Saavedra-Pellitero et al., 2019). Type A is mostly restricted to the northern SAZ, but it is occasionally present in the PFZ in the Drake Passage (Figs. 3, 4) and it is the only type within morphogroup A in this study. Morphotypes belonging to the *E. huxleyi* morphogroup B (which includes morphotypes B, B/C, C and O) are present in the SAZ and the PFZ, but they disappear south of the PF. Morphometric measurements on coccoliths of *E. huxleyi* from the selected samples show that the length of types A, B/C-C and O overlap in both transects (Fig. 5). In the Drake Passage, coccolith lengths range from 2.86 to 3.96 ± 0.43 μm (unless specified, ± refers to the SD from now on) with a mean average of 3.49 ± 0.33 μm for A type (including normal and overcalcified specimens), 2.87 to 4.11 ± 0.45 μm for B type, 2.20 to 3.98 ± 0.37 μm for B/C-C types, 2.42 to 4.16 ± 0.41 μm for O type, and an average of 2.98 ± 0.40 μm for morphogroup B. In the New Zealand transect, maximum lengths range from 2.25 to 3.59 μm, with an average of 2.95 ± 0.28 μm for *E. huxleyi* type A, 1.95 to 3.62 ± 0.33 μm for B/C-C types, 2.07 to 4.14 ± 0.36 μm for type O, and an average of 2.87 ± 0.35 μm for morphogroup B.

Figure 5 provides a latitudinal overview of morphometric data compared to the (averaged) degree of calcification (indicated by the dimensionless relative tube width index; Young et al., 2014). In the New Zealand transect there are no significant changes in coccolith lengths except for a wide scatter of values characterizing the size class distribution of each sample. This feature reflects the large variability in coccolith size as observed on coccoliths from a single coccosphere (Fig. 2e). However, in the Drake Passage transect, *E. huxleyi* coccoliths are notably larger offshore of Chile (Fig. 5a).

Emiliania huxleyi masses calculated in the New Zealand transect range from 0.61 to 2.93 pg with an average of 1.47 ± 0.46 pg per coccolith within morphogroup A, and from 0.36 to 2.86 pg, with an average of 1.15 ± 0.43 pg per placolith from morphogroup B (Fig. 3e). In the Drake Passage, the masses per coccolith for morphogroup A are almost double that in the New Zealand transect, varying between 1.39 pg and 6.26 pg, with an average of 3.00 ± 1.19 pg. The placolith masses in morphogroup B range from 0.57 to 3.75 pg with a mean of 1.44 ± 0.62 pg across the Drake Passage (Fig. 4e). The coccolith-estimated PICs for just the species *E. huxleyi* are generally lower in the New Zealand transect (average morphogroup A: 0.015 ± 0.005 pmol and B: 0.011 ± 0.004 pmol per coccolith, mean including both morphogroups = 1.19 ± 0.44 pmol per coccolith) than in the in the Drake Passage (average morphogroup A: 0.030 ± 0.012 pmol and B: 0.014 ± 0.007 pmol per coccolith, mean including both morphogroups = 1.66 ± 0.91 pmol per coccolith). Across both transects, the average coccolith mass for *E. huxleyi* in the study area is 1.35 ± 0.69 pmol per coccolith (Table 5).

We observed that some coccoliths are clearly overcalcified (see Fig. 5), with a thick inner tube (up to 0.76 µm in sample PS97/018-1) that extends into the central area. Specimens belonging to morphogroup A show a higher degree of calcification than those belonging to morphogroup B, resulting not only in a thicker inner tube but also in thicker distal shield T-elements. The overcalcified coccospheres co-occur with normally calcified coccospheres, but they are restricted to the northernmost samples (Fig. 5). The relative tube width, calculated using equation 2, varies from 0.10 to 0.28 ± 0.04 in morphogroup A and from 0.07 to 0.21 ± 0.03 in morphogroup B for the New Zealand transect. Values are higher in the Drake Passage, ranging from 0.05 to 0.50 ± 0.12 for *E. huxleyi* morphogroup A, and from 0.02 to 0.22 ± 0.04 for morphogroup B. The degree of calcification is highly variable within each sample of the New Zealand transect (Fig. 3d), but overcalcified specimens (relative tube width >0.23), typically represented by type A, only occur in the northernmost samples (Fig. 5b). The averaged relative tube width index shows increased values not only in the SAZ offshore of New Zealand, but also around 54°S and in the PFZ (Figs. 3d, 5b), which points to a certain degree of variation in the calcification within morphotypes BC/C and O. A more marked N-S decrease in the relative tube width values is observed in the Drake Passage, with notably higher values offshore of Chile (Figs. 4d and 5a), where relatively large and heavily calcified type A coccospheres are present.

4.2 Coccolith-estimated PIC and satellite-derived PIC

Emiliania huxleyi dominates the coccolithophore assemblage in the study area, with abundances of $1.4x10^5$ coccospheres/L (at station TR033) south of the SAF in the New Zealand transect and $1.5x10^5$ coccospheres/L (at station PS97/034-2) in the Drake Passage SAZ (Malinverno et al., 2015; Saavedra-Pellitero et al., 2019), and it is also the main contributor to sea-surface PIC (Figs. 3 and 4). *Calcidiscus leptoporus* (mostly the intermediate-sized form) is the secondmost abundant species and makes significant contributions to the coccolithophore PIC at certain locations (up to $1.4x10^4$ cells/L in the New Zealand transect and $1.4x10^3$ cells/L in the Drake Passage, Figs. 3 and 4) (Malinverno et al., 2015; Saavedra-Pellitero et al., 2019). *Calcidiscus leptoporus* generally represents on average 20.2% of the total coccolithophore PIC in the New Zealand transect and 5.3% in the Drake Passage but can occasionally reach maximum PIC contributions of 68.3% (at station TR008, in the SAZ) and of 31.1% (at station PS97/017-1, in the SAZ) (Figs. 1, 6).

A minor contribution from less abundant or rare species is found in the northern SAZ of both transects, where diversity is higher (for species list see Malinverno et al., 2015; Saavedra-Pellitero et al., 2019), with a poleward decreasing trend and almost no contribution south of the SAF (Fig. 6). *Emiliania huxleyi* is responsible for almost all of the coccolith-estimated PIC in the PFZ, but its contribution decreases at the PF (in the Drake Passage) and Southern ACC Front (in the New Zealand transect, ca. 63.7°S) and further south. Daily, weekly and monthly satellite (MODIS-Aqua)-derived PIC at the sampling locations are generally higher than coccolith-estimated PIC in both transects; this difference is larger in the Drake Passage (Fig. 4) than in the New Zealand transect (Fig. 3). There are discrepancies in absolute values, in addition to the already inherent variations in the weekly compared to the monthly PIC estimates and the limited availability of L2 data. These are particularly obvious at the PF (ca. 60°S in the Drake Passage) or to the south of it (ca. 62.5°S in the New Zealand transect), where the

satellite-derived and coccolith-estimated PIC become decoupled, characterized by high reflectance in the satellite data but no coccolithophores in the AZ (Figs. 7 and 8).

5. Discussion

5.1 PIC variability in the SAZ and PFZ

In the studied transects, the coccolith-estimated PIC and the satellite-derived PIC show a comparable trend in the SAZ and PFZ, but there is a strong discrepancy in the AZ (Fig. 7). The fact that coccolith-estimated PIC is generally lower than satellite-derived PIC in the SAZ and PFZ (Figs. 3, 4 and 7) could be due to an underestimation of the calculated species-specific coccolith PIC. The potential assumptions linked to the coccolith-estimated PIC, including shape factors (*Ks*), average coccolith length (*L*), number of coccoliths per coccosphere, and/or number of coccolith layers per cell (Table 3), have associated uncertainties. Although we have tried to minimize these errors by measuring the actual coccolith size range and counting the number of coccoliths per coccosphere (rather than using assumed values), the total error can still add up to ± 15%, and even ± 50% (Young and Ziveri, 2000; Figs. 3 and 4). Additionally, the fact that the difference between coccolith-estimated PIC and satellite-derived PIC is greater in the Drake Passage transect than in the New Zealand transect may also be partly due to the fact that detached coccoliths (in addition to coccospheres) were only included in the estimates for the New Zealand transect. Given that *E. huxleyi* is the dominant species and the main contributor to coccolith-estimated PIC in the SAZ and PFZ of both transects (Fig. 6), we focused on its abundance, morphotype distribution, morphometrics and calcite mass per coccolith to assess potential PIC discrepancies. Overall, our morphometric data from selected samples along the New Zealand and Drake Passage transects show (1) differences in calcification between the different *E. huxleyi* morphotypes, which are particularly evident in type A (Figs. 3, 4, and 6), (2) a large scatter of relative tube width within morphotypes and within each sample, particularly pronounced in the New Zealand transect (Figs. 3, 5), and (3) a slight decreasing trend in coccolith size and degree of calcification in the Drake Passage (Figs. 4, 5), which is not observed in the New Zealand transect. This suggests that environmental influences have no significant effect on the degree of calcification but clearly control the distribution of *E. huxleyi* morphotypes (which are genetically-determined; Bendif et al., 2023) and thus indirectly affect the coccolith mass variation. This could also explain the southwards decreasing trend in calcification in the Drake Passage, as the relatively large and heavily calcified type A coccospheres occur almost exclusively in the northern parts of both transects.

Coccolith-estimated PIC for *E. huxleyi* are generally in agreement with the calcite content per coccolith obtained by Balch et al. (2014) and Poulton et al. (2011) along the Patagonian Shelf, as well as by Charalampopoulou et al. (2016) off southern Chile (Table 5). However, our *E. huxleyi* PIC estimates are generally higher than those estimated by Charalampopoulou et al. (2016) in the rest of the Drake Passage. Our values are slightly lower than those obtained by Rigual Hernández et al. (2020a)

in the Australian and New Zealand sectors of the SO, those from the same latitudinal range in the Indian SO by Beaufort et al. (2011), and coccolith-based PIC values obtained by Valença et al. (2024) using various methodologies in laboratory-cultured specimens (Table 5). Our *E. huxleyi* PIC estimates are also notably lower than the values obtained by Saavedra-Pellitero et al. (2019), who used circularly polarized light plus the C-Calcita software developed by Fuertes et al. (2014) across the Drake Passage (Fig. 9a). The mass estimates by Saavedra-Pellitero et al. (2019) for the same samples, for which an average mass of 4.64 ± 2.53 pg (i.e. 0.0464 ± 0.0253 pmol per coccolith) was assumed for *E. huxleyi* (n = 796) without distinguishing between different morphotypes (Fig. 9c), are 2.8 times higher than in our current study (Table 5). We extrapolated the potential contribution of the remaining coccolithophore taxa by this factor (i.e., multiplied by 2.8 the PIC values calculated in this study for *C. leptoporus* and minor species) (Fig. 9c). Both N-S coccolith mass and PIC trends mirror each other, showing that both methods are valid for tracking PIC variations, but the C-Calcita-derived PICs tend to overestimate satellite-derived PIC values, except in a couple of locations. This can be attributed to the calibration of the coccolith thickness within the software C-Calcita, which has been improved in recent years with the use of a calcite wedge instead of a calcareous spine (e.g. Guitián et al., 2022). The generally higher mass coccolith values using polarised light microscopy compared to morphometric approaches in the same sample set have already been observed in previous studies (e.g. Rigual Hernández et al., 2020a), but due to recent technical developments the results from these two methods are becoming more comparable (e.g. Valença et al., 2024).

In the AZ (south of about 62.5°S in the New Zealand transect and about 60°S in the Drake Passage), high reflectance is detected by remote sensing but is not associated with a coccolithophore bloom (Figs. 3, 4 and 7). Concentrations of *E. huxleyi*, which show maximum numbers in the PFZ on the New Zealand transect and moderate values in the Drake Passage, drop southward of this location on the Southern ACC Front and the PF (Malinverno et al., 2015; 2016). Satellite data show the different impact of ACC fronts on the distribution of *E. huxleyi* (Holligan et al., 2010): in the Drake Passage, where the fronts are strictly constrained by topography, *E. huxleyi* is bounded by the PF to the south (Saavedra-Pellitero et al., 2019), while in the eastern Scotia Sea, where the ACC fronts are broadly separated, *E. huxleyi* spreads between the PF and the Southern ACC Front (Holligan et al., 2010; Poulton et al., 2011; Poulton et al., 2013). This pattern also emerges from the compilation by Malinverno et al. (2016), which shows that the Southern ACC Front marks the southern boundary in different SO sectors. Occasional occurrences of *E. huxleyi* south of the Southern ACC Front have been documented south of Tasmania and in the Weddell Sea in certain years by conventional micropalaeontological observations (e.g. Winter et al., 1999; Cubillos et al., 2007), as well as in the Australian sector of the SO and in the Scotia Sea using surface reflectance data only (Holligan et al., 2010; Winter et al., 2014). However, in our study, *E. huxleyi* is constrained by the Southern ACC Front, corresponding to a maximum sea surface temperature of 1°C in the New Zealand transect.

The different taxonomic considerations of *E. huxleyi* in different studies make it difficult to compare and combine data, especially in light of recent advances in the field. Given the dominance of this taxa in the SO, a key area for global warming and ocean acidification studies, the efforts of the scientific calcareous nannofloral community should focus on a more

standardized classification of *E. huxleyi* morphotypes. However, differentiation and recognition of the various morphotypes is time consuming and tedious and plays only a minor role in the calculation of the total coccolithophorid PIC, as observed in other areas of the SO (e.g. Rigual Hernández et al., 2020a, b). The changes in mass within the B morphotype (which includes types B/C-C, C, O) in the two transects are negligible in the PIC calculation, while a differentiation into morphogroups A and B still has an influence on the calculation of PIC. Specimens of *E. huxleyi* belonging to morphogroup A only occur in the northern areas of both transects, where they play a limited role together with the PIC input from other massive species such as *C. leptoporus* (Fig. 6). Overall, the changes in total coccolithophore-PIC in the study area are caused by the abundance and occurrence within the entire coccolithophore community, rather than the different carbonate masses or the southward changes in morphotype composition along both SO transects. The relative contribution of the different *E. huxleyi* A and B morphogroups to the coccolithophore-PIC in the SO deserves further exploration in light of the rapid development of remote sensing and recent evolution of machine learning approaches for PIC estimates.

5.2 Assessing potential biases in PIC estimates for the AZ

The generally higher satellite-derived PIC numbers compared to the coccolith-estimated PIC values in the SAZ and PFZ (Figs. 3, 4, and 7) could also be due to the presence of other carbonate-forming organisms (and/or their fragments). For example, foraminifera can contribute to a significant fraction of the total PIC in the SO south of Australia, especially between 55-60°S (Trull et al., 2018). We do not have data for the Drake Passage, but planktonic foraminifera were observed in the filter samples across the New Zealand transect, showing increased abundance (together with the tintinnid species *Codonellopsis pusilla*) in the PFZ (see Malinverno et al., 2016 for further details). Although foraminifera and other hard-shelled micro-zooplankton PIC particles provide negligible backscatter per unit mass (Balch et al., 1996), they can be a source of error in the PIC volume calculation when considering only coccolithophores. Assessing the significance of carbonate-forming organisms relative to other taxa in the SO is an important topic but falls beyond the scope of this paper.

In addition to the described challenges in calculating species-specific coccolith PICs, the observed discrepancies between satellite-derived PIC values and coccolith-estimated PIC values may also result from a combination of several other factors related to the sensitivities and limitations of the PIC algorithm (Mitchell et al., 2017; Balch and Mitchell, 2023; NASA Ocean Biology Processing Group, 2023), differences in spatial and temporal resolution (Table 4), and environmental factors (e.g. turbidity or other particulate matter that can affect the accuracy of satellite-derived PIC estimates). MODIS-derived L2 PIC data was limited due to the cloudy skies of the SO during the sampling period (see Figs. 1S and 2S in the Supplementary Material). To mitigate the impact of these data gaps in our analysis, we extended the time window for data extraction to several days and computed the mean for each location, whilst also using L3 products. This approach could obscure potential variability at shorter temporal scales and create discrepancies when comparing with sample measurements taken on specific days. The fact that the overall trends are comparable in the New Zealand and Drake Passage transects (Fig. 7) could also suggest a satellite bias linked to the algorithm. We are aware that the MODIS-Aqua Ocean Color was re-processed in 2022 to incorporate

updates in instrument calibration, new ancillary sources and algorithm improvements (NASA Ocean Biology Processing Group, 2023), but the validation of the PIC measurements was based on a low number of in-situ measurements compared to other products (e.g. 1347 in situ measurements for chlorophyll a and just 42 for PIC, all of them in the Atlantic Ocean; NASA Ocean Biology Processing Group, 2023). The differences in PIC could also be due to the fact that we are comparing in situ values to weekly and monthly averages, as well as also smoothing data by considering averaged values when calculating coccolith-estimated PIC (especially length and number of coccoliths per coccosphere). In addition, sampling at slightly different times of the year may also have an influence on the PIC values determined (Rigual Hernández et al., 2018; Rigual-Hernández et al., 2020a, b).

Considering the differences in the two SO transects studied here, which were sampled 11 years apart, we could assume that surface coccolith-estimated PIC (up to 20 m water depth) underestimates satellite-derived PIC concentrations in the SAZ and PFZ. This discrepancy is evident in our data, where coccolith-estimated PIC concentrations calculated using different methodologies, such as C-Calcita, exceed those obtained from the satellite data. This indicates that there is still a need for improved precision and accuracy in coccolith-estimated PIC concentration methods. Therefore, it is crucial to refine existing methods and develop new algorithms to enhance both precision as well as accuracy.

The magnitude and spectral characteristics of water-leaving radiance detected by satellites are influenced by the inherent properties of the optically active constituents. These include: (1) light scattering by PIC, other biogenic particles or lithogenic material (e.g. Bi et al., 2023), as well as (2) light absorption by phytoplankton biomass (i.e., chlorophyll a concentration) and dissolved organic matter (e.g. Reynolds et al., 2001; Ferreira et al., 2009). The strong correlation between high values of water-leaving radiance and high *E. huxleyi* PIC concentrations has been successfully proven in bloom areas (e.g. Gordon et al., 1988; Balch et al., 2005; Holligan et al., 2010; Balch et al., 2011; Balch et al., 2014; Balch and Mitchell, 2023; Oliver et al., 2023). However, not all bright waters are caused by *E. huxleyi* blooms, as shown by Broerse et al. (2003) in the Bering Sea, Balch et al. (2007) in the Gulf of Maine, and Daniels et al. (2012) in the Bay of Biscay. Suspended particles, which include either reworked coccoliths, lithogenic material or empty diatom frustules, could be responsible for high values of water-leaving radiance, at least in nearshore regions (Broerse et al., 2003; Balch and Mitchell, 2023).

The occurrence of bright waters along the studied transects should theoretically be constrained by the position of the PF/ Southern ACC Front. Malinverno et al. (2015; 2016) showed a significant shift in the community composition from carbonate to silica-dominated microfossils in the New Zealand transect at the Southern ACC Front, with diatoms being the most abundant mineralized phytoplankton group in the transect (Fig. 3k). Coccolithophores disappear south of the Southern ACC Front, and the composition of the siliceous phytoplankton changes from a dominance of large diatoms (*Fragilariopsis kerguelensis*) in the north to a dominance of small diatoms (such as the cold adapted *Fragilariopsis cylindrus*) in the south, with a notable increase in spiny silicoflagellates (e.g. *Stephanocha speculum* var. *coronata*) and small siliceous plankton (Parmales, Archaeomonads) (Malinverno et al., 2016) coincident with high values of chlorophyll a in the AZ (Figs. 3l, 8). Extant diatoms

have not yet been studied in the exact same water samples collected during PS97 Expedition. However, the abundance of fossil diatoms in surface sediments in the Drake Passage shows an increase south of the PF, along with an increase in the relative abundance of siliciclastics and biogenic opal (Cárdenas et al., 2018). This contrasts with the relatively low satellite-derived chlorophyll a concentration in the AZ (Fig. 4k), but this only due to the very limited number of daily L2 data available. *Fragilariopsis kerguelensis* appears to dominate up to the Southern ACC Front, and *F. cylindrus* is found south of this front, in colder waters of the Drake Passage (Cárdenas et al., 2018).

Different alternatives have been suggested for the high reflectance in the AZ of the SO, such as microbubbles (mostly during storms), floating loose ice, high concentrations of other particulate matter such as glacial flour (especially close to the Antarctic continent) or *Phaeocystis* blooms (Balch et al., 2011; Balch, 2018; Balch and Mitchell, 2023). Our observations do not allow us to comprehensively determine the potential causes of this high reflectance, but we note that a high abundance of small opal biogenic particles, such as small-size diatoms, silicoflagellates and siliceous plankton observed (as well as their fragments) would be consistent with the observed high scattering of these waters at least in the New Zealand transect (Figs. 1, 3, 4, 3S and 4S in Supplementary Material), even though opal particles have a much lower refractive index than calcite (Balch, 2009; Costello et al., 1995).

The satellite-derived and coccolith-estimated PIC discrepancies observed in this work emphasize the importance of in situ measurements and sampling. This also highlights the need for further investigation of the factors influencing water-leaving radiance and the reliability of remote sensing estimates, especially south of the PF. Future research should focus on refining methodologies and satellite algorithms to improve the accuracy of PIC estimates and better understand the dynamics of coccolithophores, as well as phytoplankton and calcifying micro-zooplankton communities more generally in the Pacific sector of the SO (especially compared to other sectors). Such efforts will enhance our understanding of carbon cycling and its impact on marine ecosystems at high latitudes.

6 Conclusions

The comparison between particulate inorganic carbon (PIC) derived from satellite data and coccolithophore-morphometric-based estimates in two transects of the Pacific sector of the Southern Ocean (separated in time and space) demonstrates the limited availability of high-quality satellite-derived data (mostly due to atmospheric conditions), and the need for refining methodologies to accurately produce coccolith-estimated PIC. Based on our data the following conclusions can be drawn:

1) *Emiliania huxleyi* is the predominant coccolithophore species contributing the most to the total sea-surface coccolith-PIC in the New Zealand transect (mainly sampled in 2005) and as well as in the Drake Passage (sampled in 2016).

Calcidiscus leptoporus may occasionally contribute significantly to the total coccolithophore-PIC at certain locations, whereas the rest of the coccolithophore taxa contribute only marginally in the studied areas.

2) *Emiliania huxleyi* consists of several morphotypes, which have different, partly overlapping geographical distributions. The relatively massive type A morphogroup occurs in the northern Subantarctic Zone (SAZ) and occasionally in the Polar Front Zone (PFZ) of the Drake Passage, while specimens of the less calcified morphogroup B (which includes types B, B/C, C and O) occur in the SAZ and the PFZ of both transects. Neither the slightly different carbonate masses nor the southward changes in morphotype composition have a decisive influence on the coccolith-estimated PIC, which is mostly determined by the abundance of *E. huxleyi* in this area.
3) The drop in abundance of *E. huxleyi* morphogroup B in the Antarctic Zone (AZ) marks the southernmost extent of coccolithophores, occuring at the PF in the Drake Passage and the Southern ACC Front in the New Zealand transect. This boundary is not recognizable using satellite-derived PIC values.
4) We found that satellite-derived PIC values and coccolith-estimated PIC values follow a comparable trend in the SAZ and PFZ. However, satellite-derived PIC values are generally higher than coccolith-estimated PIC. This difference could be due to a lack of precision in the coccolith-based PIC estimates, to the presence of foraminifera and/or other hard-shelled calcifying micro-zooplankton adding potential error when calculating total PIC volume, or to a certain bias in the algorithm due to the low number of measurements used for the validation of the satellite-derived PIC calibration.
5) There is an observed decoupling of satellite-derived PIC and coccolith-estimated PIC south of the Polar Front (PF), in the AZ. Despite having high satellite reflectance values, no coccolithophores were observed in this area of high chlorophyll a concentration. We are unable to determine the reason for this with our data, but note that an abundance of small biogenic opal particles, such as small-size diatoms, silicoflagellates and/or siliceous plankton (as well as their fragments) or, potential biogenic particles not visible in scanning electron microscope (e.g. *Phaeocystis* aggregations, microbubbles, etc.) could possibly provide an explanation for this observation.

The observed discrepancies between satellite-derived and coccolith-estimated PIC south of the PF highlight the importance of in situ measurements for improving PIC estimates based on coccolith morphometrics and polarizing light microscopy. In combination with further refinements of remote sensing methods, this will allow a better understanding of the dynamics of coccolithophores, phytoplankton and calcifying micro-zooplankton communities in the Pacific sector of the Southern Ocean.

Data Availability Statement

The authors confirm that the data from which the findings of this study are available within the article Supplementary Materials and are stored in the data repository https://pangaea.de/ (https://doi.pangaea.de/10.1594/PANGAEA.964672 and https://doi.pangaea.de/10.1594/PANGAEA.964674).

Author contributions

The study was designed by EM, MSP and KHB. EM and NMV carried out the morphometric measurements and classified the specimens of *E. huxleyi*. EM and MSP calculated coccolith-PICs, plotted the data and wrote an earlier version of the manuscript. NB-J and HL provided remote sensing data for the study area, and were actively involved in the discussion of the findings as well as in the writing of the paper. All authors approved the submitted version.

Competing interests

The authors declare that they have no conflict of interest.

Acknowledgements

Satellite-derived Particulate Inorganic Carbon (PIC) data was downloaded from the Ocean Color Web Level 1 & 2 Browser (https://oceancolor.gsfc.nasa.gov/cgi/browse.pl?sen) and Level 3 & 4 Browser (https://oceancolor.gsfc.nasa.gov/l3), both of them services provided by NASA's Ocean Biology Distributed Active Archive Centre (OB.DAAC).
The authors acknowledge the use of the JASMIN (Joint Analysis System for the Met Office, NERC, and UKRI) (https://jasmin.ac.uk/) Jupyter Notebook service to process the satellite-derived PIC data. We would like to express our gratitude to the JASMIN team for their support and the valuable resources they provide to the scientific community.
The authors are grateful to two anonymous reviewers, to Prof. Peter von Dassow and to the handling associate editor, Prof. Jamie Shutler, for their invaluable suggestions on a previous version of the paper. The Alfred Wegener Institute Bremerhaven provided part of the plankton samples required for this study. Dr. Frank Lamy, Dr. Hartmut Schulz, *R/V Polarstern* officers and crew are thanked for their help during the PS97 Expedition.
Dr. Amanda Frigola (Barcelona Supercomputing Center, Spain), Dr. Ute Merkel (University of Bremen/MARUM, Germany) and Dr. Mark Hardiman (University of Portsmouth, UK) are acknowledged for their help with remote sensing data collection advice. Dr. Nick Pepin (University of Portsmouth, UK) and Dr. Barney Balch (Bigelow Laboratory for Ocean Sciences, USA) are thanked for their comments and suggestions on this piece of research during the "Advances in Coccolithophore research" meeting. Dr. Julio Saavedra (RIP) is thanked for his continuous encouragement to finish up this paper.

Financial support

This research was supported by the University of Portsmouth, by the Deutsche Forschungsgemeinschaft with a grant to Karl-Heinz Baumann (reference number: BA 1648/30-1) -through previous funding for Mariem Saavedra-Pellitero and Nele M. Vollmar- and by the MIUR project “Dipartimenti di Eccellenza 2018/2023" for Elisa Malinverno, at the Department of Earth and Environmental Sciences, University of Milano-Bicocca. The University of Portsmouth Research and Innovation Services, as well as Copernicus Publications are acknowledged for their additional financial support to publish this paper as Open Access.

References

Babin, M., Morel, A., Fournier-Sicre, V., Fell, F., and Stramski, D.: Light scattering properties of marine particles in coastal and open ocean waters as related to the particle mass concentration, Limnology and Oceanography, 48, 843-859, doi: 10.4319/lo.2003.48.2.0843, 2003a.

Babin, M., Stramski, D., Ferrari, G. M., Claustre, H., Bricaud, A., Obolensky, G., and Hoepffner, N.: Variations in the light absorption coefficients of phytoplankton, nonalgal particles, and dissolved organic matter in coastal waters around Europe, Journal of Geophysical Research: Oceans, 108, doi: 10.1029/2001JC000882, 2003b.

Bailey, S. W., & Werdell, P. J., A multi-sensor approach for the on-orbit validation of ocean color satellite data products, Rem. Sens. Environ., 102, 12-23, 2006.

Balch, W. M.: The Ecology, Biogeochemistry, and Optical Properties of Coccolithophores, Annual Review of Marine Science, 10, 71-98, doi: 10.1146/annurev-marine-121916-063319, 2018.

Balch, W. M., Holligan, P. M., Ackleson, S. G., and Voss, K. J.: Biological and optical properties of mesoscale coccolithophore blooms in the Gulf of Maine, Limnology and Oceanography, 36, 629-643, doi: 10.4319/lo.1991.36.4.0629, 1991.

Balch, W. M., Kilpatrick, K. A., Holligan, P., Harbour, D., and Fernandez, E.: The 1991 coccolithophore bloom in the central North Atlantic. 2. Relating optics to coccolith concentration, Limnology and Oceanography, 41, 1684-1696, 1996.

Balch, W. M., Drapeau, D. T., Cucci, T. L., Vaillancourt, R. D., Kilpatrick, K. A., and Fritz, J. J.: Optical backscattering by calcifying algae: Separating the contribution of particulate inorganic and organic carbon fractions, Journal of Geophysical Research: Oceans, 104, 1541-1558, doi: 10.1029/1998JC900035, 1999.

Balch, W. M., Gordon, H. R., Bowler, B. C., Drapeau, D. T., and Booth, E. S.: Calcium carbonate measurements in the surface global ocean based on Moderate-Resolution Imaging Spectroradiometer data, Journal of Geophysical Research: Oceans, 110, doi: 10.1029/2004JC002560, 2005.

Balch, W. M., Drapeau, D. T., Bowler, B. C., Booth, E. S., Windecker, L. A., and Ashe, A.: Space–time variability of carbon standing stocks and fixation rates in the Gulf of Maine, along the GNATS transect between Portland, ME, USA, and Yarmouth, Nova Scotia, Canada, Journal of Plankton Research, 30, 119-139, doi: 10.1093/plankt/fbm097, 2007.

Balch, W. M., Drapeau, D. T., Bowler, B. C., Lyczskowski, E., Booth, E. S., and Alley, D.: The contribution of coccolithophores to the optical and inorganic carbon budgets during the Southern Ocean Gas Exchange Experiment: New evidence in support of the "Great Calcite Belt" hypothesis, Journal of Geophysical Research: Oceans, 116, doi: 10.1029/2011jc006941, 2011.

Balch, W. M., Drapeau, D. T., Bowler, B. C., Lyczkowski, E. R., Lubelczyk, L. C., Painter, S. C., and Poulton, A. J.: Surface biological, chemical, and optical properties of the Patagonian Shelf coccolithophore bloom, the brightest waters of the Great Calcite Belt, Limnology and Oceanography, 59, 1715-1732, doi: 10.4319/lo.2014.59.5.1715, 2014.

Balch, W. M., Bates, N. R., Lam, P. J., Twining, B. S., Rosengard, S. Z., Bowler, B. C., Drapeau, D. T., Garley, R., Lubelczyk, L. C., Mitchell, C., and Rauschenberg, S.: Factors regulating the Great Calcite Belt in the Southern Ocean and its biogeochemical significance, Global Biogeochemical Cycles, 30, 1124-1144, doi: 10.1002/2016gb005414, 2016.

Balch, W. M., and Mitchell, C.: Remote sensing algorithms for particulate inorganic carbon (PIC) and the global cycle of PIC, Earth-Science Reviews, 239, 104363, doi: 10.1016/j.earscirev.2023.104363, 2023.

Balch, W. M., and P.E. Utgoff: Potential interactions among ocean acidification, coccolithophores, and the optical properties of seawater, Oceanography and Marine Biology Annual Review, 22, 146-159, doi: 10.5670/oceanog.2009.104, 2009.

Baumann, K.-H.: Importance of coccolith size measurements for carbonate estimations. Micropaleontology, 50 (1), 35-43, 2004.

Beaufort, L.: Weight estimates of coccoliths using the optical properties (birefringence) of calcite, Micropaleontology, 51, 289–298, 2005.

Beaufort, L., Probert, I., de Garidel-Thoron, T., Bendif, E. M., Ruiz-Pino, D., Metzl, N., Goyet, C., Buchet, N., Coupel, P., Grelaud, M., Rost, B., Rickaby, R. E. M., and de Vargas, C.: Sensitivity of coccolithophores to carbonate chemistry and ocean acidification, Nature, 476, 80-83, doi: 10.1038/nature10295, 2011.

Bendif, E. M., Probert, I., Archontikis, O. A., Young, J. R., Beaufort, L., Rickaby, R. E., and Filatov, D.: Rapid diversification underlying the global dominance of a cosmopolitan phytoplankton, The ISME Journal, 17, 630-640, doi: 10.1038/s41396-023-01365-5, 2023.

Beuvier, T., Probert, I., Beaufort, L., Suchéras-Marx, B., Chushkin, Y., Zontone, F., and Gibaud, A.: X-ray nanotomography of coccolithophores reveals that coccolith mass and segment number correlate with grid size, Nature Communications, 10, 751, doi: 10.1038/s41467-019-08635-x, 2019.

Bevington, P. R., Data Reduction and Error Analysis for the Physical Sciences, 336 pp., McGraw-Hill, 1969

Bi, S., Hieronymi, M., and Röttgers, R.: Bio-geo-optical modelling of natural waters, Frontiers in Marine Science, 10, doi: 10.3389/fmars.2023.1196352, 2023.

Bollmann, J.: Technical Note: Weight approximation of coccoliths using a circular polarizer and interference colour derived retardation estimates - (The CPR Method), Biogeosciences, 11, 1899-1910, doi: 10.5194/bg-11-1899-2014, 2014.

Broerse, A. T. C., Tyrrell, T., Young, J. R., Poulton, A. J., Merico, A., Balch, W. M., and Miller, P. I.: The cause of bright waters in the Bering Sea in winter, Continental Shelf Research, 23, 1579-1596, doi: 10.1016/j.csr.2003.07.001, 2003.

Cárdenas, P., Lange, C. B., Vernet, M., Esper, O., Srain, B., Vorrath, M.-E., Ehrhardt, S., Müller, J., Kuhn, G., Arz, H. W., Lembke-Jene, L., and Lamy, F.: Biogeochemical proxies and diatoms in surface sediments across the Drake Passage reflect oceanic domains and frontal systems in the region, Progress in Oceanography, doi: 10.1016/j.pocean.2018.10.004, 2018.

Charalampopoulou, A., Poulton, A. J., Bakker, D. C. E., Lucas, M. I., Stinchcombe, M. C., and Tyrrell, T.: Environmental drivers of coccolithophore abundance and calcification across Drake Passage (Southern Ocean), Biogeosciences, 13, 5917-5935, doi:10.5194/bg-13-5917-2016, 2016.

Costello, D. K., Carder, K. L., and Hou, W.: Aggregation of diatom bloom in a mesocosm: Bulk and individual particle optical measurements, Deep Sea Research Part II: Topical Studies in Oceanography, 42, 29-45, doi: 10.1016/0967-0645(95)00003-9, 1995.

Cubillos, J. C., Wright, S. W., Nash, G., de Salas, M. F., Griffiths, B., Tilbrook, B., Poisson, A., and Hallegraeff, G. M.: Calcification morphotypes of the coccolithophorid *Emiliania huxleyi* in the Southern Ocean: changes in 2001 to 2006 compared to historical data, Marine Ecology Progress Series, 348, 47-54, doi: 10.3354/meps07058, 2007.

Daniels, C. J., Tyrrell, T., Poulton, A. J., and Pettit, L.: The influence of lithogenic material on particulate inorganic carbon measurements of coccolithophores in the Bay of Biscay, Limnology and Oceanography, 57, 145-153, doi: 10.4319/lo.2012.57.1.0145, 2012.

de Baar, H. J. W., de Jong, J. T. M., Bakker, D. C. E., Loscher, B. M., Veth, C., Bathmann, U., and Smetacek, V.: Importance of iron for plankton blooms and carbon dioxide drawdown in the Southern Ocean, Nature, 373, 412-415, doi: 10.1038/373412a0, 1995.

Devred, E., Sathyendranath, S., Stuart, V., Maass, H., Ulloa, O., and Platt, T.: A two-component model of phytoplankton absorption in the open ocean: Theory and applications, Journal of Geophysical Research: Oceans, 111, doi: 10.1029/2005JC002880, 2006.

European Space Agency. ESA Sentinel Application Platform (SNAP) 9.0.0. https://step.esa.int/main/snap-9-0-released/, 2022.

Ferreira, A., Garcia, V. M. T., and Garcia, C. A. E.: Light absorption by phytoplankton, non-algal particles and dissolved organic matter at the Patagonia shelf-break in spring and summer, Deep Sea Research Part I: Oceanographic Research Papers, 56, 2162-2174, doi: 10.1016/j.dsr.2009.08.002, 2009.

Fuertes, M.-Á., Flores, J.-A., and Sierro, F. J.: The use of circularly polarized light for biometry, identification and estimation of mass of coccoliths, Marine Micropaleontology, 113, 44-55, doi: 10.1016/j.marmicro.2014.08.007, 2014.

GEBCO Compilation Group: GEBCO_2022 Grid. Data set available online from the British Oceanographic Data Centre, Liverpool, UK. doi: 10.5285/e0f0bb80-ab44-2739-e053-6c86abc0289c, 2022.

Gordon, A. L., Molinelli, E., and Baker, T.: Large-scale relative dynamic topography of the Southern Ocean, Journal of Geophysical Research: Oceans, 83, 3023-3032, doi: 10.1029/JC083iC06p03023, 1978.

Gordon, H. R., Brown, O. B., Evans, R. H., Brown, J. W., Smith, R. C., Baker, K. S., and Clark, D. K.: A semianalytic radiance model of ocean color, Journal of Geophysical Research: Atmospheres, 93, 10909-10924, doi: 10.1029/JD093iD09p10909, 1988.

Gordon, H. R., Boynton, G. C., Balch, W. M., Groom, S. B., Harbour, D. S., and Smyth, T. J.: Retrieval of coccolithophore calcite concentration from SeaWiFS Imagery, Geophysical Research Letters, 28, 1587-1590, doi: 10.1029/2000GL012025, 2001.

Gravalosa, J. M., Flores, J.-A., Sierro, F. J., and Gersonde, R.: Sea surface distribution of coccolithophores in the eastern Pacific sector of the Southern Ocean (Bellingshausen and Amundsen Seas) during the late austral summer of 2001, Marine Micropaleontology, 69, 16-25, doi: 10.1016/j.marmicro.2007.11.006, 2008.

Guitián, J., Fuertes, M. Á., Flores, J. A., Hernández-Almeida, I., and Stoll, H.: Variation in calcification of Reticulofenestra coccoliths over the Oligocene–Early Miocene, Biogeosciences, 19, 5007-5019, doi: 10.5194/bg-19-5007-2022, 2022.

Harlay, J., Borges, A. V., Van Der Zee, C., Delille, B., Godoi, R. H. M., Schiettecatte, L. S., Roevros, N., Aerts, K., Lapernat, P. E., Rebreanu, L., Groom, S., Daro, M. H., Van Grieken, R., and Chou, L.: Biogeochemical study of a coccolithophore bloom in the northern Bay of Biscay (NE Atlantic Ocean) in June 2004, Progress in Oceanography, 86, 317-336, doi: 10.1016/j.pocean.2010.04.029, 2010.

Holligan, P. M., Viollier, M., Harbour, D. S., Camus, P., and Champagne-Philippe, M.: Satellite and ship studies of coccolithophore production along a continental shelf edge, Nature, 304, 339-342, doi: 10.1038/304339a0, 1983.

Holligan, P. M., Fernández, E., Aiken, J., Balch, W. M., Boyd, P., Burkill, P. H., Finch, M., Groom, S. B., Malin, G., Muller, K., Purdie, D. A., Robinson, C., Trees, C. C., Turner, S. M., and van der Wal, P.: A biogeochemical study of the coccolithophore, *Emiliania huxleyi*, in the North Atlantic, Global Biogeochemical Cycles, 7, 879-900, doi: 10.1029/93gb01731, 1993.

Holligan, P. M., Charalampopoulou, A., and Hutson, R.: Seasonal distributions of the coccolithophore, *Emiliania huxleyi*, and of particulate inorganic carbon in surface waters of the Scotia Sea, Journal of Marine Systems, 82, 195-205, doi: 10.1016/j.jmarsys.2010.05.007, 2010.

Klaas, C. and Archer, D. E.: Association of sinking organic matter with various types of mineral ballast in the deep sea: Implications for the rain ratio, Global Biogeochemical Cycles, 16, 1116, https://doi.org/10.1029/2001GB001765, 2002.

Kleijne, A.: Morphology, taxonomy and distribution of extant coccolithophores (calcareous nannoplankton), Ph.D., Vrije Universiteit, Amsterdam, 321 pp., 1993.

Klinck, J., and Nowlin, W. D.: Antarctic Circumpolar Current, in: Encyclopedia of Ocean Sciences, edited by: Steele, J. H., Academic Press, Oxford, 151-159, 2001.

Lamy, F.: The Expedition PS97 of the Research Vessel POLARSTERN to the Drake Passage in 2016, edited by: Lamy, F., Berichte zur Polar- und Meeresforschung, Reports on Polar and Marine Research, 167 pp., https://doi.org/10.2312/BzPM_0701_2016, 2016.

669 Malinverno, E., Triantaphyllou, M. V., and Dimiza, M. D.: Coccolithophore assemblage distribution along a temperate to polar
670 gradient in theWest Pacific sector of the Southern Ocean (January 2005) Micropaleontology, 61, 489-506, 2015.
671 Malinverno, E., Maffioli, P., and Gariboldi, K.: Latitudinal distribution of extant fossilizable phytoplankton in the Southern
672 Ocean: Planktonic provinces, hydrographic fronts and palaeoecological perspectives, Marine Micropaleontology, 123,
673 41-58, doi: 10.1016/j.marmicro.2016.01.001, 2016.
674 Mitchell, C., Hu, C., Bowler, B., Drapeau, D., and Balch, W. M.: Estimating Particulate Inorganic Carbon Concentrations of
675 the Global Ocean From Ocean Color Measurements Using a Reflectance Difference Approach, Journal of Geophysical
676 Research: Oceans, 122, 8707-8720, doi: 10.1002/2017JC013146, 2017.
677 Mohan, R., Mergulhao, L. P., Guptha, M. V. S., Rajakumar, A., Thamban, M., AnilKumar, N., Sudhakar, M., and Ravindra,
678 R.: Ecology of coccolithophores in the Indian sector of the Southern Ocean, Marine Micropaleontology, 67, 30-45, doi:
679 10.1016/j.marmicro.2007.08.005, 2008.NASA Goddard Space Flight Center, Ocean Ecology Laboratory, Ocean Biology
680 Processing Group. Moderate-resolution Imaging Spectroradiometer (MODIS) Aqua Level-2 Ocean Color, Version 2022
681 Data; NASA OB.DAAC, Greenbelt, MD, USA. doi: 10.5067/AQUA/MODIS/L2/OC/2022, 2022a [Accessed on 10 July
682 2024].
683 NASA Goddard Space Flight Center, Ocean Ecology Laboratory, Ocean Biology Processing Group: Moderate-resolution
684 Imaging Spectroradiometer (MODIS) Aqua Level-3 Mapped Particulate Inorganic Carbon, Version 2022 Data; NASA
685 OB.DAAC, Greenbelt, MD, USA. doi: 10.5067/AQUA/MODIS/L3M/PIC/2022, 2022b [Access 01 June 2023].
686 NASA Ocean Biology Processing Group: Particulate Inorganic Carbon (PIC). Available from
687 https://oceancolor.gsfc.nasa.gov/resources/atbd/pic/, 2023 [Access 14 June 2023].
688 Neukermans, G., Oziel, L., and Babin, M.: Increased intrusion of warming Atlantic water leads to rapid expansion of temperate
689 phytoplankton in the Arctic, Global Change Biology, 24, 2545-2553, doi: 10.1111/gcb.14075, 2018.
690 Okada, H., and McIntyre, A.: Modern coccolithophores of the Pacific and North Atlantic oceans, Micropaleontology, 23, 1-
691 54, doi: 10.2307/1485309 1977.
692 Oliver, H., McGillicuddy, D. J., J., Krumhardt, K. M., Long, M. C., Bates, N. R., Bowler, B. C., Drapeau, D. T., and Balch,
693 W. M.: Environmental drivers of coccolithophore growth in the Pacific sector of the Southern Ocean, Global
694 Biogeochemical Cycles, 37(11), https://doi.org/10.1029/2023GB007751, 2023.
695 Orsi, A. H., and Harris, U.: Fronts of the Antarctic Circumpolar Current - GIS data, Ver. 1, Australian Antarctic Data Centre
696 - https://data.aad.gov.au/metadata/records/antarctic_circumpolar_current_fronts, 2019 [Access 26 May 2023].
697 Orsi, A. H., Whitworth III, T., and Nowlin Jr, W. D.: On the meridional extent and fronts of the Antarctic Circumpolar Current,
698 Deep Sea Research Part I: Oceanographic Research Papers, 42, 641-673, doi: 10.1016/0967-0637(95)00021-w, 1995.
699 Poulton, A. J., Young, J. R., Bates, N. R., and Balch, W. M.: Biometry of detached *Emiliania huxleyi* coccoliths along the
700 Patagonian Shelf, Marine Ecology Progress Series, 443, 1-17, doi: 10.3354/meps09445, 2011.

Poulton, A. J., Painter, S. C., Young, J. R., Bates, N. R., Bowler, B., Drapeau, D., Lyczsckowski, E., and Balch, W. M.: The 2008 *Emiliania huxleyi* bloom along the Patagonian Shelf: Ecology, biogeochemistry, and cellular calcification, Global Biogeochemical Cycles, 27, 1023-1033, doi: 10.1002/2013GB004641, 2013.

Reynolds, R. A., Stramski, D., and Mitchell, B. G.: A chlorophyll-dependent semianalytical reflectance model derived from field measurements of absorption and backscattering coefficients within the Southern Ocean, Journal of Geophysical Research: Oceans, 106, 7125-7138, doi: 10.1029/1999JC000311, 2001.

Rigual Hernández, A. S., Flores, J. A., Sierro, F. J., Fuertes, M. A., Cros, L., and Trull, T. W.: Coccolithophore populations and their contribution to carbonate export during an annual cycle in the Australian sector of the Antarctic zone, Biogeosciences, 15, 1843-1862, BG, 2018.

Rigual Hernández, A. S., Trull, T. W., Nodder, S. D., Flores, J. A., Bostock, H., Abrantes, F., Eriksen, R. S., Sierro, F. J., Davies, D. M., Ballegeer, A. M., Fuertes, M. A., and Northcote, L. C.: Coccolithophore biodiversity controls carbonate export in the Southern Ocean, Biogeosciences, 17, 245-263, doi: 10.5194/bg-17-245-2020, 2020a.

Rigual-Hernández, A. S., Trull, T. W., Flores, J. A., Nodder, S. D., Eriksen, R., Davies, D. M., Hallegraeff, G. M., Sierro, F. J., Patil, S. M., Cortina, A., Ballegeer, A. M., Northcote, L. C., Abrantes, F., and Rufino, M. M.: Full annual monitoring of Subantarctic *Emiliania huxleyi* populations reveals highly calcified morphotypes in high-CO_2 winter conditions, Scientific reports, 10, 2594, doi: 10.1038/s41598-020-59375-8, 2020b.

Rivero-Calle, S., Gnanadesikan, A., Del Castillo, C. E., Balch, W. M., and Guikema, S. D.: Multidecadal increase in North Atlantic coccolithophores and the potential role of rising CO_2, Science, 350, 1533-1537, doi: 10.1126/science.aaa8026, 2015.

Robertson, J. E., Robinson, C., Turner, D. R., Holligan, P., Watson, A. J., Boyd, P., Fernandez, E., & Finch, M., The impact of a coccolithophore bloom on oceanic carbon uptake in the northeast Atlantic during summer 1991, Deep-Sea Research Part I, 41(2), 297-314, doi:10.1016/0967-0637(94)90005-1, 1994.

Rost, B., and Riebesell, U.: Coccolithophore calcification and the biological pump: response to environmental changes, in: Coccolithophores: from molecular processes to global impact, edited by: Thierstein, H. R., and Young, J. R., Springer, Berlin-Heidelberg, Germany, 99-125, 2004.

Saavedra-Pellitero, M., Baumann, K.-H., Flores, J.-A., and Gersonde, R.: Biogeographic distribution of living coccolithophores in the Pacific sector of the Southern Ocean, Marine Micropaleontology, 109, 1-20, doi: 10.1016/j.marmicro.2014.03.003, 2014.

Saavedra-Pellitero, M., Baumann, K. H., Fuertes, M. Á., Schulz, H., Marcon, Y., Vollmar, N. M., Flores, J. A., and Lamy, F.: Calcification and latitudinal distribution of extant coccolithophores across the Drake Passage during late austral summer 2016, Biogeosciences, 16, 3679-3702, doi: 10.5194/bg-16-3679-2019, 2019.

Salter, I., Schiebel, R., Ziveri, P., Movellan, A., Lampitt, R., and Wolff, G. A.: Carbonate counter pump stimulated by natural iron fertilization in the Polar Frontal Zone, Nature Geoscience, 7, 885-889, doi: 10.1038/ngeo2285, 2014.

Samtleben, C. and Schröder, A.: Living coccolithophore communities in the Norwegian-Greenland Sea and their record in sediments, Marine Micropaleontology, 19, 333-354, 1992.

Schindelin, J., Arganda-Carreras, I., Frise, E., Kaynig, V., Longair, M., Pietzsch, T., Preibisch, S., Rueden, C., Saalfeld, S., Schmid, B., Tinevez, J.-Y., White, D. J., Hartenstein, V., Eliceiri, K., Tomancak, P., and Cardona, A.: Fiji: an open-source platform for biological-image analysis, Nature Methods, 9, 676-682, doi: 10.1038/nmeth.2019, 2012.

Schneider, C. A., Rasband, W. S., and Eliceiri, K. W.: NIH Image to ImageJ: 25 years of image analysis, Nature Methods, 9, 671-675, doi: 10.1038/nmeth.2089, 2012.

Shutler, J. D., Land, P. E., Brown, C. W., Findlay, H. S., Donlon, C. J., Medland, M., Snooke, R., and Blackford, J. C.: Coccolithophore surface distributions in the North Atlantic and their modulation of the air-sea flux of CO_2 from 10 years of satellite Earth observation data, Biogeosciences, 10, 2699-2709, doi: 10.5194/bg-10-2699-2013, 2013.

Smyth, T. J., Moore, G. F., Groom, S. B., Land, P. E., and Tyrrell, T.: Optical modeling and measurements of a coccolithophore bloom, Appl. Opt., 41, 7679-7688, doi: 10.1364/AO.41.007679, 2002.Trull, T. W., Passmore, A., Davies, D. M., Smit, T., Berry, K., and Tilbrook, B.: Distribution of planktonic biogenic carbonate organisms in the Southern Ocean south of Australia: a baseline for ocean acidification impact assessment, Biogeosciences, 15, 31-49, doi: 10.5194/bg-15-31-2018, 2018.

Tyrrell, T., and Taylor, A. H.: A modelling study of *Emiliania huxleyi* in the NE atlantic, Journal of Marine Systems, 9, 83-112, doi:10.1016/0924-7963(96)00019-X, 1996.

Valença, C. R., Beaufort, L., Hallegraeff, G. M., and Müller, M. N.: Technical note: A comparison of methods for estimating coccolith mass, Biogeosciences, 21, 1601–1611, https://doi.org/10.5194/bg-21-1601-2024, 2024.

Vollmar, N. M., Baumann, K.-H., Saavedra-Pellitero, M., and Hernández-Almeida, I.: Distribution of coccoliths in surface sediments across the Drake Passage and calcification of *Emiliania huxleyi* morphotypes, Biogeosciences, 19, 585–612, https://doi.org/10.5194/bg-19-585-2022, 2022.

Werdell, J., O'Reilly, J., Hu, C., Feng, L., Lee, Z., Franz, B., Bailey, S., Proctor, C., and Wang, G.: Chlorophyll a. NASA Algorithm Publication Tool, 2023-11-06, v1.1. Available from https://www.earthdata.nasa.gov/documents/chlor-a/v1.1, 2023, https://doi.org/10.5067/JCQB8QALDOYD [Access 20 July 2024]

Whitworth, T. I.: Zonation and geostrophic flow of the Antarctic circumpolar current at Drake Passage, Deep Sea Research Part A. Oceanographic Research Papers, 27, 497-507, doi: 10.1016/0198-0149(80)90036-9, 1980.

Winter, A., Elbrächter, M., and Krause, G.: Subtropical coccolithophores in the Weddell Sea, Deep Sea Research Part I: Oceanographic Research Papers, 46, 439-449, doi: 10.1016/S0967-0637(98)00076-4, 1999.

Winter, A., Henderiks, J., Beaufort, L., Rickaby, R. E. M., and Brown, C. W.: Poleward expansion of the coccolithophore *Emiliania huxleyi*, Journal of Plankton Research, 36, 316-325, 10.1093/plankt/fbt110, 2014.

Yang, T. N., and Wei, K. Y.: How many coccoliths are there in a coccosphere of the extant coccolithophorids? A compilation, Journal of Nannoplankton Research, 25, 7-15, 2003.

Young, J.: Coccobiom2 Macros, available from: http://ina.tmsoc.org/nannos/coccobiom/Usernotes.html, 2015 [Access 23 August 2017]

Young, J. R., and Ziveri, P.: Calculation of coccolith volume and it use in calibration of carbonate flux estimates, Deep Sea Research Part II: Topical Studies in Oceanography, 47, 1679-1700, doi: 10.1016/S0967-0645(00)00003-5, 2000.

Young, J., Bown, P., and Lees, J.: Nannotax3 Website, International Nannoplankton Association, available at: http://www.mikrotax.org/Nannotax3/, 2023 [Access 05 July 2023].

Young, J., Geisen, M., Cros, L., Kleijne, A., Sprengel, C., Probert, I., and Ostergaard, J.: A guide to extant coccolithophore taxonomy, Journal of Nannoplankton Research Special Issue, 1, 1–125, ISSN 1210-8049, 2003.

Young, J. R., Poulton, A. J., and Tyrrell, T.: Morphology of *Emiliania huxleyi* coccoliths on the northwestern European shelf – is there an influence of carbonate chemistry?, Biogeosciences, 11, 4771-4782, doi: 10.5194/bg-11-4771-2014, 2014.

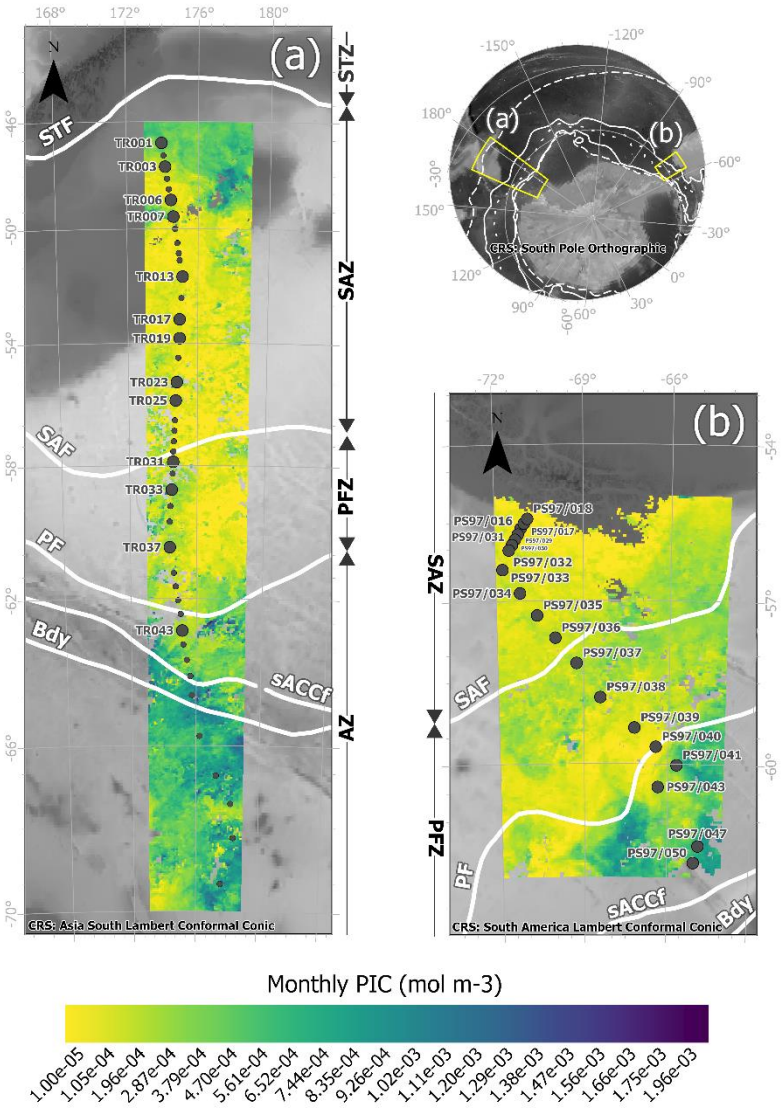

Figure 1: Study area showing the location of the water samples retrieved from (a) the New Zealand transect, collected during the XX Italian Expedition from New Zealand to Antarctica on board *R/V Italica* (December 2004-January 2005) and (b) the Drake Passage transect, collected during *Polarstern* Expedition PS97 across the Drake Passage (February-March 2016). Large dots indicate samples in which biometries on *Emiliania huxleyi* were performed, and small dots where coccolithophore census were available. The maps show MODIS-Aqua L3 PIC concentrations in mol m^{-3} g corresponding to (a) monthly mean over January 2005 and (b) monthly mean over February and March 2016, overlain on a bathymetry background (GEBCO Compilation Group, 2022). White lines indicate the average position of the Antarctic Circumpolar Current (ACC) fronts (Orsi and Harris, 2019), from north to south these are: SAF (Subantarctic Front), PF (Polar Front), sACCf (Southern ACC Front) and Bdy (Southern Boundary). The Southern Ocean zones are labeled on the side of each map: STZ, Subtropical Zone; SAZ, Subantarctic Zone; PFZ, Polar Frontal Zone; AZ, Antarctic Zone.

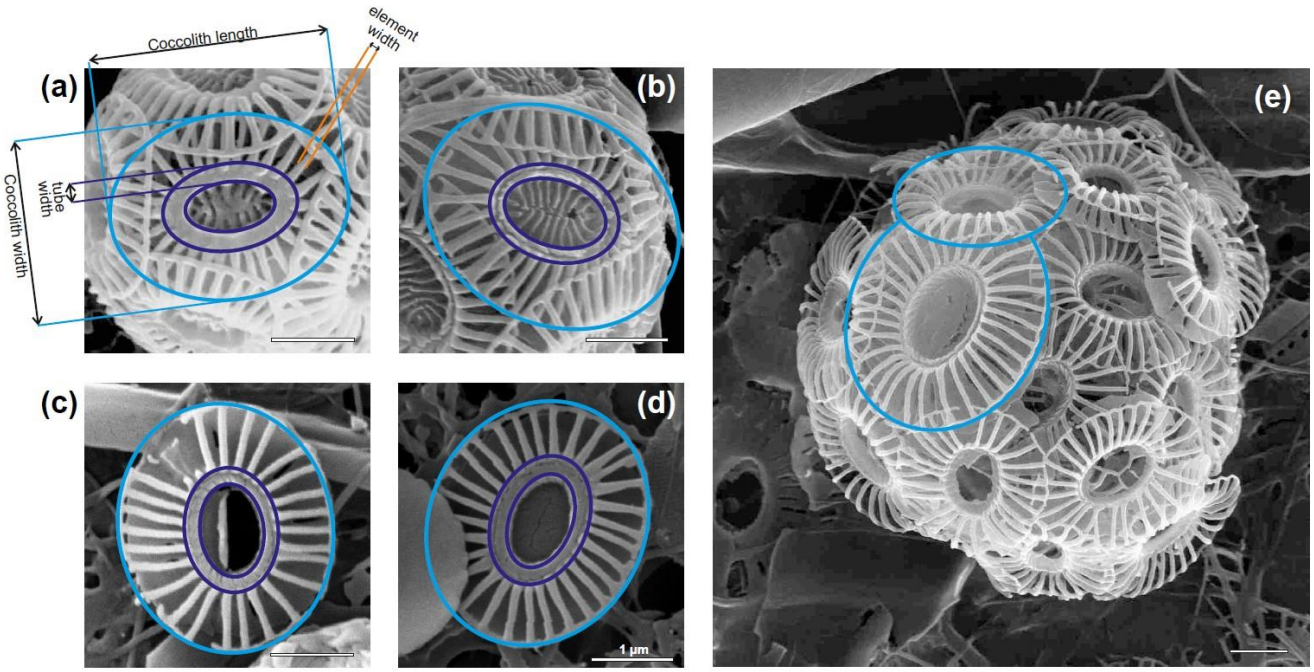

Figure 2: Parameters measured in *Emiliania huxleyi* coccoliths (a, b) type A and (c, d, e) type O in plankton samples from the New Zealand transect. Note the coccolith size variation in (e) within the same coccosphere.

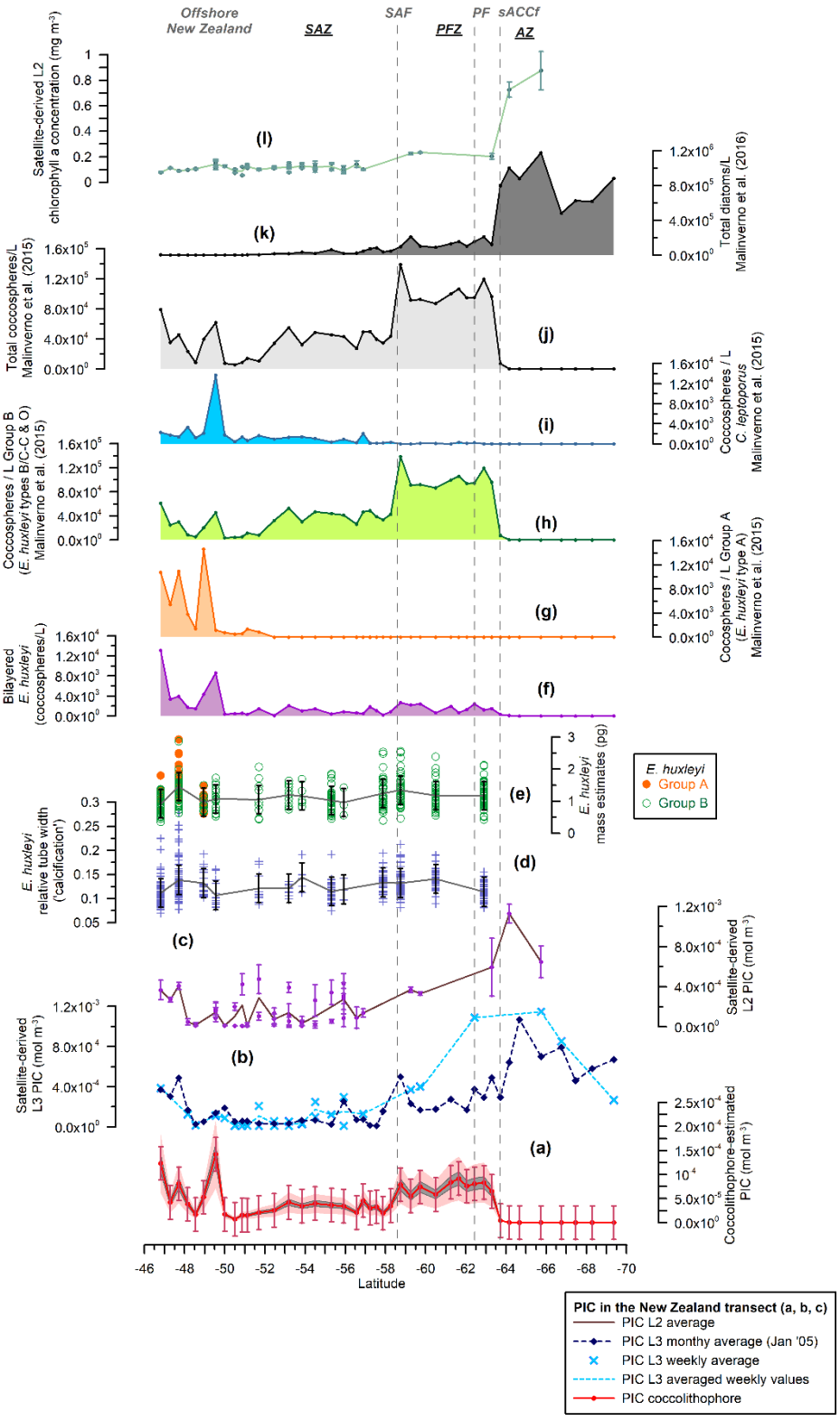
Offshore New Zealand
SAZ
SAF
PFZ
PF
sACCf
AZ
Satellite-derived L2 chlorophyll a concentration (mg m-3)
(l)
(k)
Total diatoms/L Malinverno et al. (2016)
Total coccospheres/L Malinverno et al. (2015)
(j)
Coccospheres / L C. leptoporus Malinverno et al. (2015)
Coccospheres / L Group B (E. huxleyi types B/C-C & O) Malinverno et al. (2015)
(i)
(h)
Coccospheres / L Group A (E. huxleyi type A) Malinverno et al. (2015)
(g)
Bilayered E. huxleyi (coccospheres/L)
(f)
E. huxleyi mass estimates (pg)
E. huxleyi
Group A
Group B
(e)
E. huxleyi relative tube width ('calcification')
(d)
(c)
Satellite-derived L2 PIC (mol m-3)
Satellite-derived L3 PIC (mol m-3)
(b)
(a)
Coccolithophore-estimated PIC (mol m-3)
Latitude
PIC in the New Zealand transect (a, b, c)
PIC L2 average
PIC L3 monthy average (Jan '05)
PIC L3 weekly average
PIC L3 averaged weekly values
PIC coccolithophore

795

Figure 3: New Zealand transect showing (a) estimated total coccolithophore PIC (red line with dots) in mol m^{-3}, (b) MODIS-Aqua L3 PIC concentration values (mol m^{-3}) corresponding to a monthly average (January 2005, dark blue dashed line with diamonds), weekly average (light blue dashed line with crosses), (c) MODIS-Aqua L2 PIC concentration values in mol m^{-3} (average in brown) (d) *Emiliania huxleyi* relative tube width index (average in gray), (e) *E. huxleyi* coccolith mass estimates (pg) for morphogroup A (dots) and B (circles) (average in gray), (f) number of bilayered *E. huxleyi* (coccospheres/L), (g) number of *E. huxleyi* morphogroup A (coccospheres/L), (h) number of *E. huxleyi* morphogroup B (coccospheres/L), (i) number of *Calcidiscus leptoporus* (coccospheres/L), (j) Number of total coccolithophores (coccospheres/L) (Malinverno et al., 2015), (k) Number of total diatoms (cells/L) (Malinverno et al., 2016), (l) MODIS-Aqua L2 chlorophyll a concentration in mg m^{-3}(average in light green). Note that the plankton samples were retrieved at ca. 3 m water depth. Vertical bars indicate one standard deviation on the entire population in (a), (d) and (e), and the standard deviation (considering a 5 x 5 window) in (c) and (l). The dark gray shaded area in (a) represents a 15% error and the light pink shaded area a 50% error. Vertical dashed lines indicate some of the Antarctic Circumpolar Current (ACC) fronts (Orsi and Harris, 2019): SAF (Subantarctic Front), PF (Polar Front) and sACCf (Southern ACC Front). The Southern Ocean zones are labeled as SAZ (Subantarctic Zone), PFZ (Polar Frontal Zone) and AZ (Antarctic Zone).

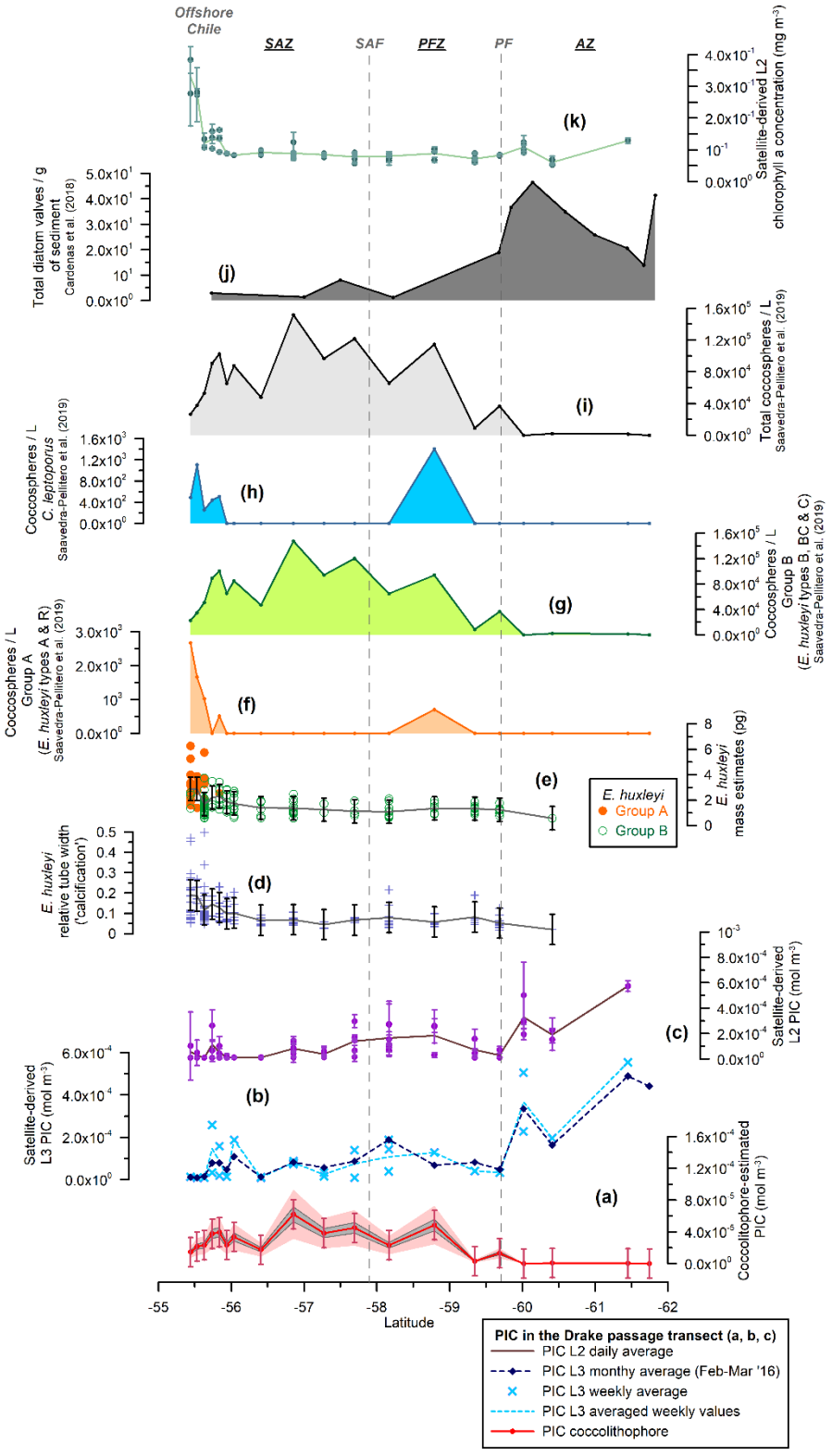
Offshore Chile
SAZ
SAF
PFZ
PF
AZ
(k)
Satellite-derived L2 chlorophyll a concentration (mg m-3)
(j)
Total diatom valves / g of sediment
Cardenas et al. (2018)
(i)
Total coccospheres / L
Saavedra-Pelliteo et al. (2019)
(h)
Coccospheres / L
C. leptoporus
Saavedra-Pelliteo et al. (2019)
(g)
Coccospheres / L
Group B
(E. huxleyi types B, BC & C)
Saavedra-Pelliteo et al. (2019)
(f)
Coccospheres / L
Group A
(E. huxleyi types A & R)
Saavedra-Pelliteo et al. (2019)
(e)
E. huxleyi
Group A
Group B
E. huxleyi mass estimates (pg)
(d)
E. huxleyi relative tube width ('calcification')
(c)
Satellite-derived L2 PIC (mol m-3)
(b)
Satellite-derived L3 PIC (mol m-3)
(a)
Coccolithophore-estimated PIC (mol m-3)
-55
-56
-57
-58
-59
-60
-61
-62
Latitude
PIC in the Drake passage transect (a, b, c)
PIC L2 daily average
PIC L3 monthy average (Feb-Mar '16)
PIC L3 weekly average
PIC L3 averaged weekly values
PIC coccolithophore

Figure 4: Drake Passage transect showing (a) estimated total coccolithophore PIC (red line with dots) in mol m^{-3}, (b) MODIS-Aqua L3 PIC concentration (mol m^{-3}) corresponding to a monthly average (February and March 2016, dark blue dashed line with diamonds), weekly average (light blue dashed line with crosses), (c) MODIS-Aqua L2 PIC concentration in mol m^{-3} (average in brown), (d) *Emiliania huxleyi* relative tube width index (average in gray), (e) *E. huxleyi* coccolith mass estimates (pg) for morphogroup A (dots) and B (circles) in (average in gray), (f) number of *E. huxleyi* morphogroup A (coccospheres/L), (g) number of *E. huxleyi* morphogroup B (coccospheres/L), (h) number of *Calcidiscus leptoporus* (coccospheres/L), (i) Number of total coccolithophores (coccospheres/L) (Saavedra-Pellitero et al., 2019), (j) Number of valves per gram of sediment from surface sediment samples across the Drake Passage and Scotia Sea (Cárdenas et al., 2018), (k) MODIS-Aqua L2 chlorophyll a concentration in mg m^{-3} (average in light green). Note that plankton samples were retrieved at 5, 10 and 20 m water depth. Vertical bars indicate one standard deviation on the entire population in (a), (d) and (e), and the standard deviation (considering a 5 x 5 window) in (c) and (k). The dark gray shaded area in (a) represents a 15% error and the light pink shaded area a 50% error. Vertical dashed lines indicate some of the Antarctic Circumpolar Current (ACC) fronts (Orsi and Harris, 2019): SAF (Subantarctic Front) and PF (Polar Front). The Southern Ocean zones are labeled as SAZ (Subantarctic Zone), PFZ (Polar Frontal Zone) and AZ (Antarctic Zone).

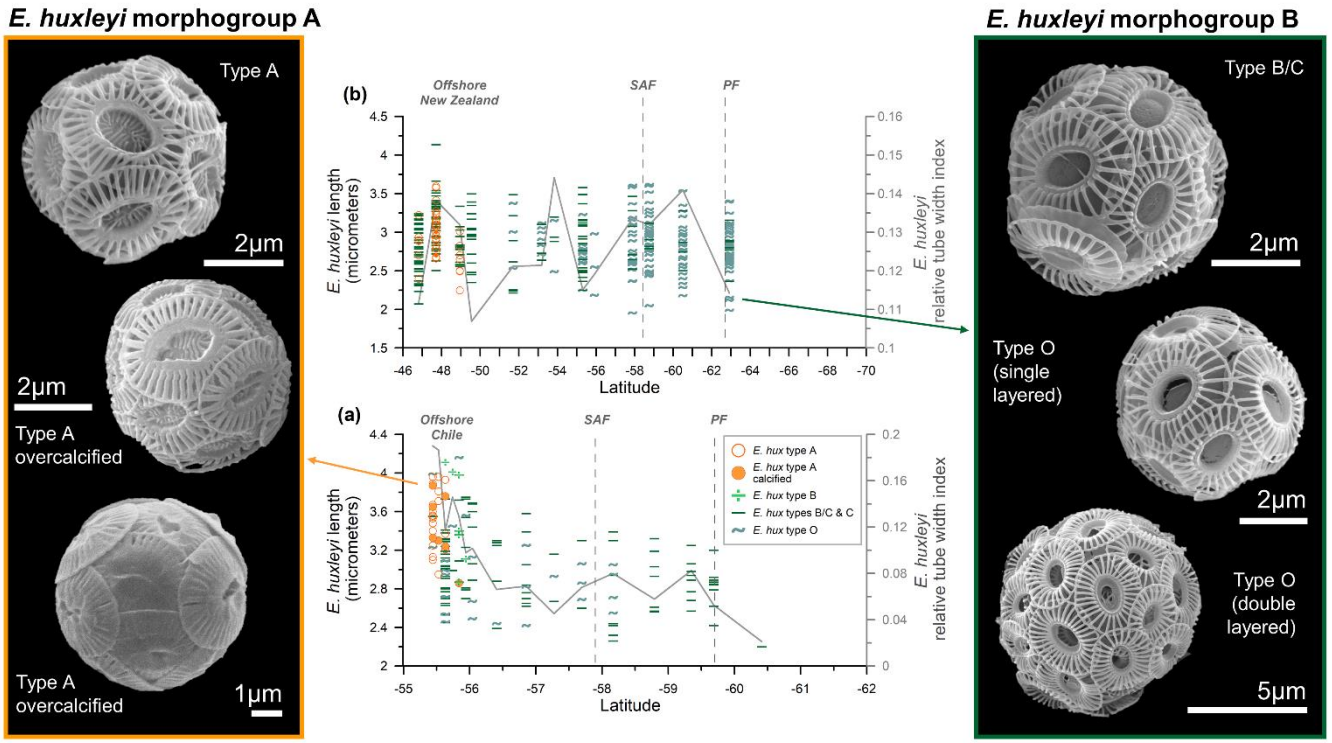

Figure 5: *Emiliania huxleyi* length (in µm) (indicated with different symbols depending on the type, and different colors depending on the morphogroup -A or B-) and averaged relative tube width index (gray line) in (a) the Drake Passage and (b) New Zealand transects. On the left-hand side: pictures of coccospheres of *E. huxleyi* type A (within the morphogroup A) showing different degrees of calcification and on the right-hand side pictures of type B/C as well as type O belonging to the morphogroup B. All the images of coccospheres are from the New Zealand transect, except for the left bottom one, which was retrieved offshore of Chile.

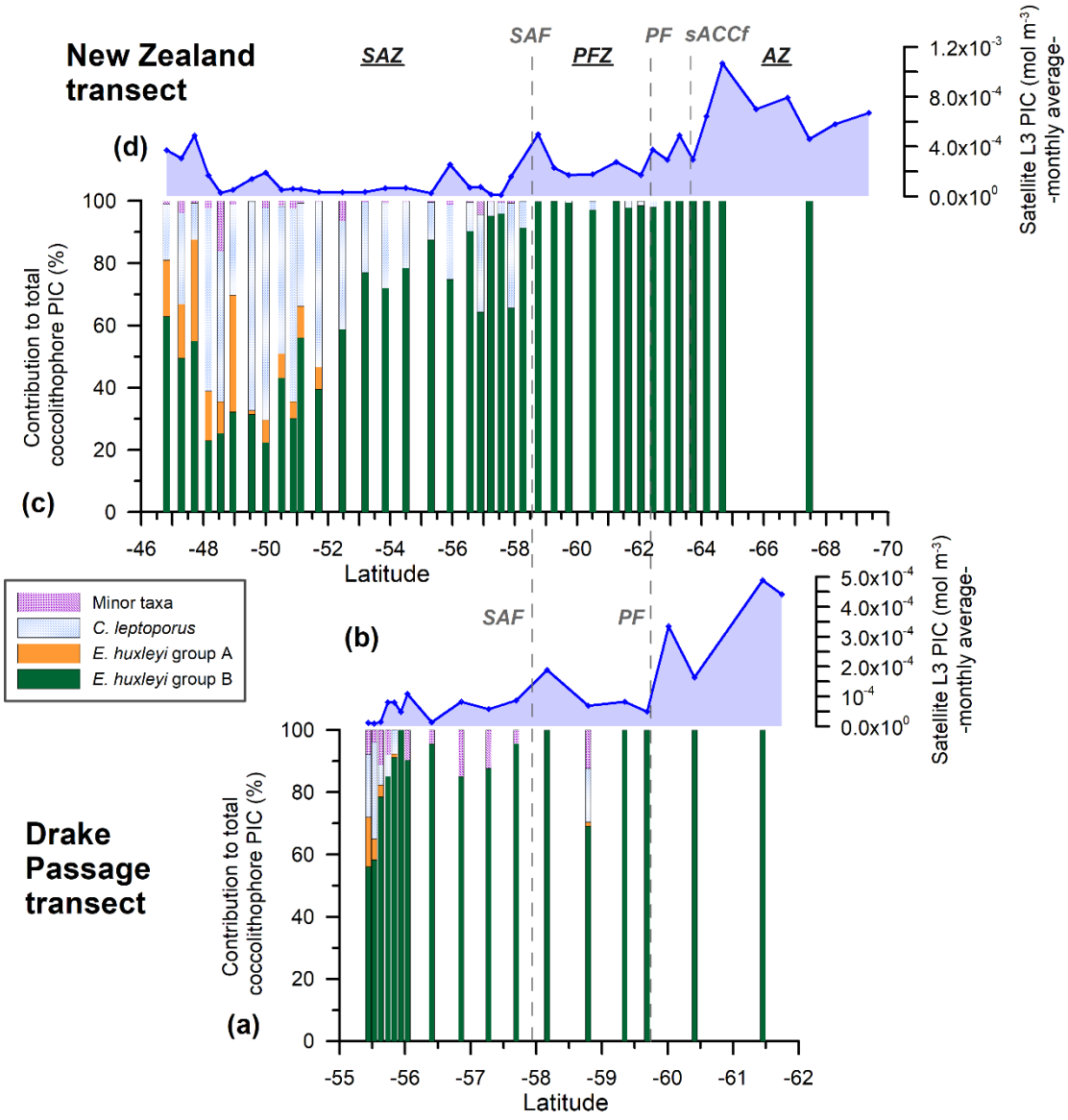

Figure 6: New Zealand (NZ) and Drake Passage (DP) transects showing (a, c) the relative PIC contribution of the different nannofloral taxa (*E. huxleyi* morphogroups A and B, *Calcidiscus leptoporus* and minor species) to the estimated coccolithophore PIC in 38 NZ and 17 DP samples bearing coccospheres; (b, d) MODIS-Aqua L3 monthly average satellite-derived PIC values (February and March 2016, dark blue line with diamonds) in mol m^{-3}. Vertical dashed lines indicate some of the Antarctic Circumpolar Current (ACC) fronts (Orsi and Harris, 2019): SAF (Subantarctic Front) and PF (Polar Front). The Southern Ocean zones are labeled as SAZ (Subantarctic Zone), PFZ (Polar Frontal Zone) and AZ (Antarctic Zone).

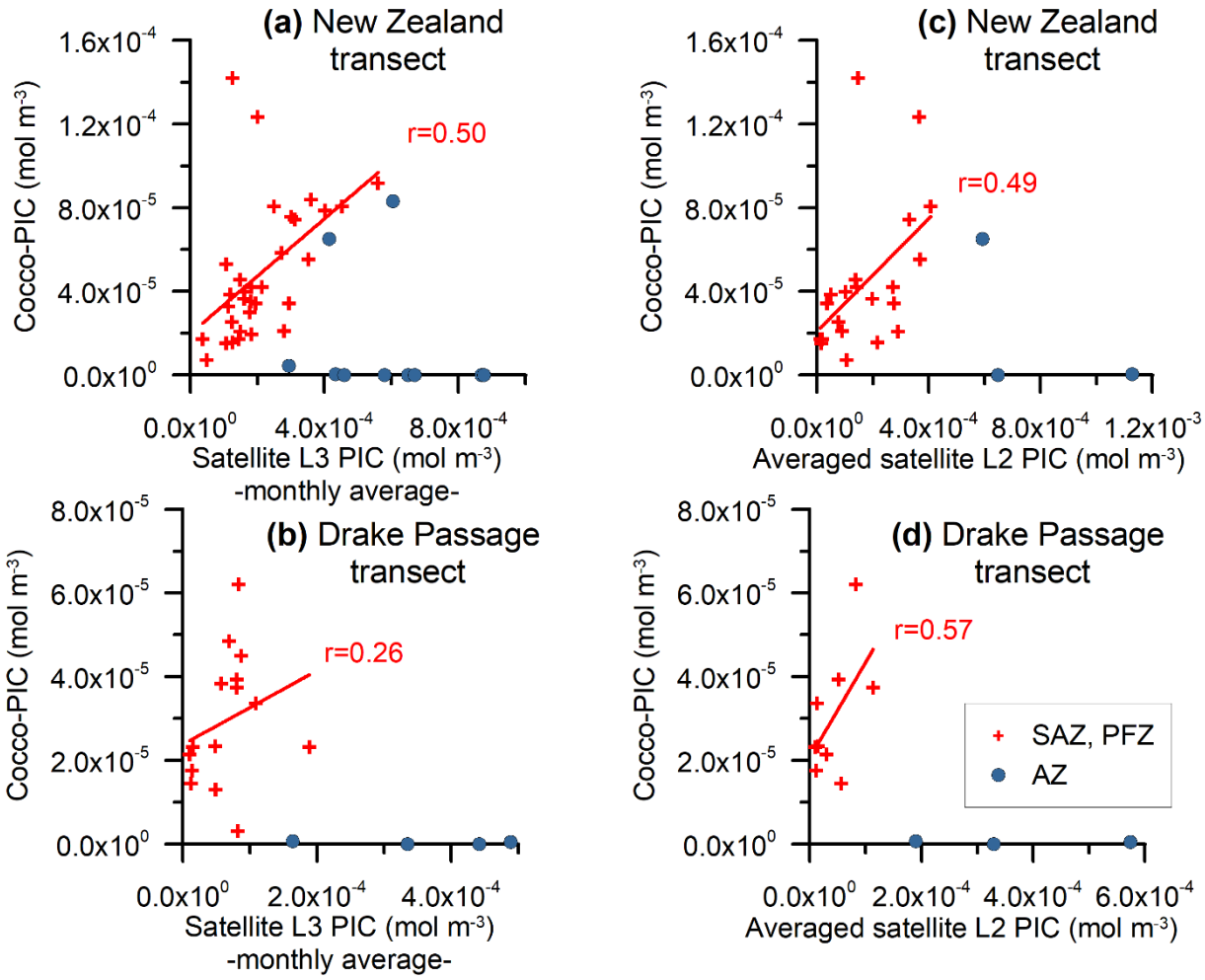

846

847 **Figure 7: Monthly MODIS-Aqua L3 PIC values versus estimated total coccolithophore PIC for (a) the New Zealand and (b) Drake**
848 **Passage transects (in mol m^{-3}). Averaged MODIS-Aqua L2 PIC values versus estimated total coccolithophore PIC for the (c) the**
849 **New Zealand and (d) Drake Passage transects (in mol m^{-3}). The samples located in the Subantarctic Zone (SAZ) and Polar Frontal**
850 **Zone (PFZ) have been indicated with crosses and those in the Antarctic Zone (AZ) with dots. A regression line and the Pearson**
851 **correlation coefficient (r) has been indicated for the samples in the SAZ and PFZ.**

852
853

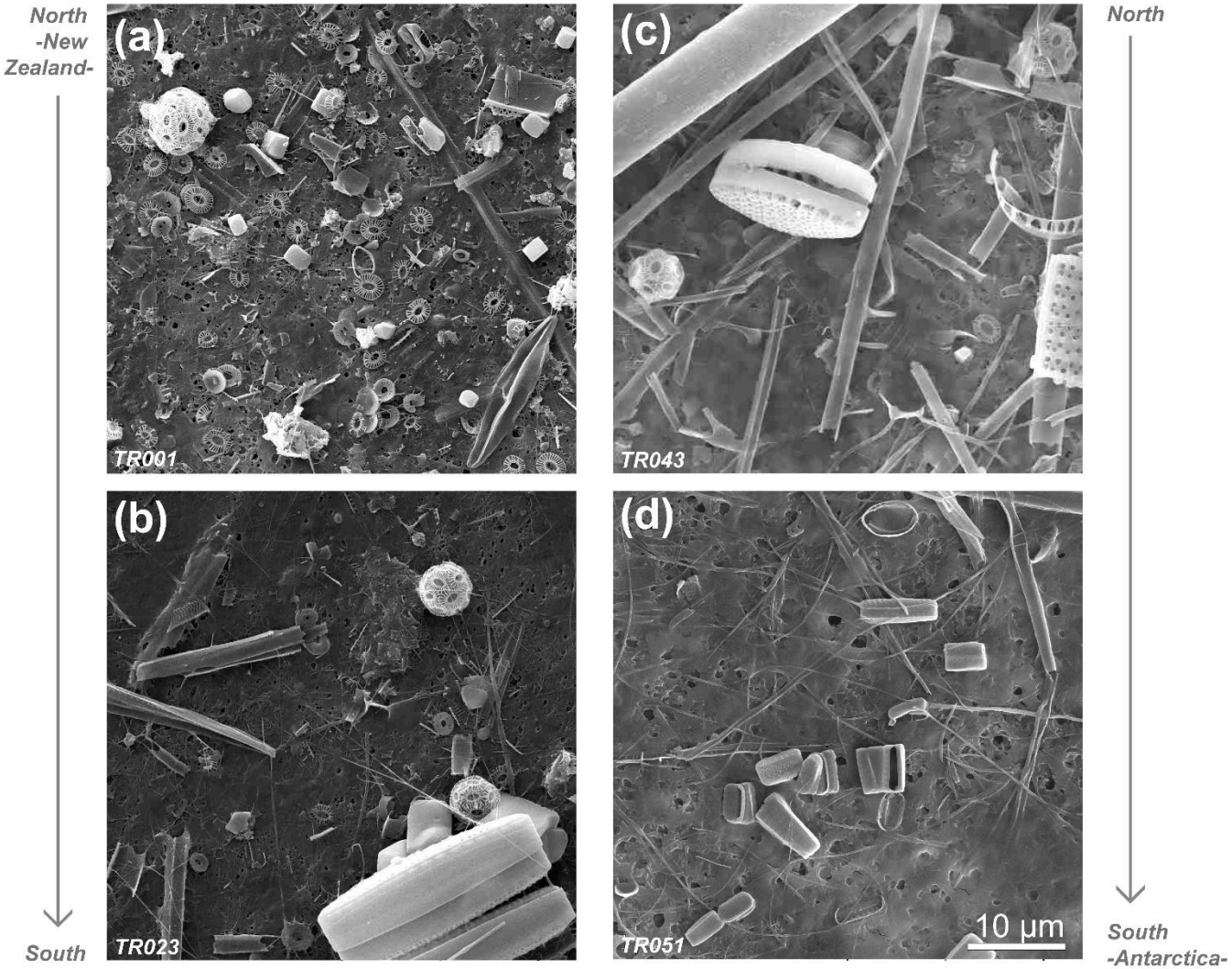

Figure 8: SEM pictures of samples retrieved in the Subantactic Zone (a, b) and south of the Polar Front (c, d) in the New Zealand transect.

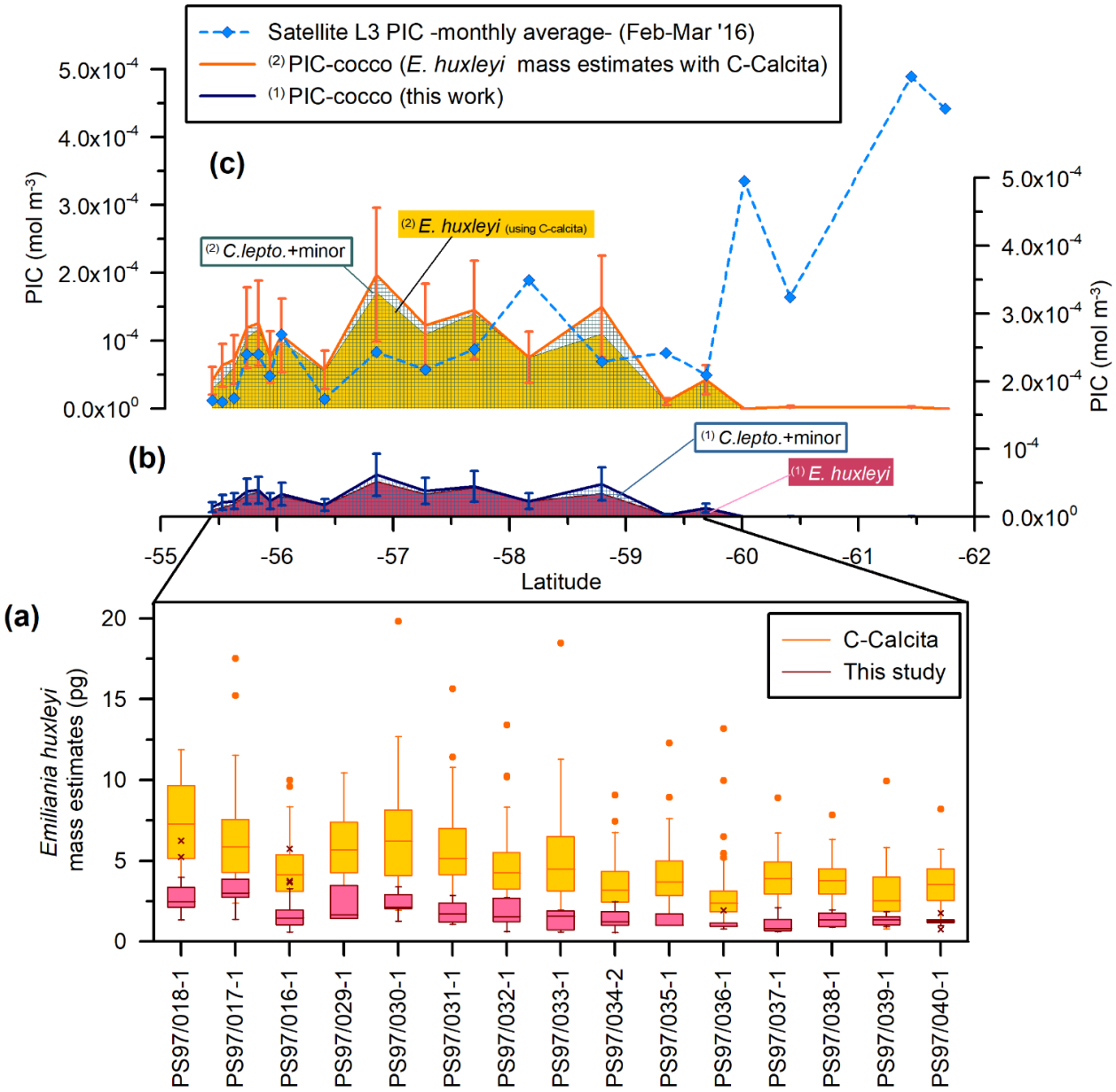

Figure 9: Drake Passage latitudinal transect showing (a) coccolith mass estimates box plots (in pg): in dark red plus pink for this study (outliers are indicated with "x") and yellow plus orange for Saavedra-Pellitero et al. (2019) (outliers are indicated with a dot); (b) estimated coccolithophore PIC (PIC-cocco) (all in mol m^{-3}) -this study)-; (c) MODIS-Aqua L3 monthly average satellite-derived PIC values (blue dashed line with diamonds) and PIC-cocco calculated considering averaged *Emiliania huxleyi* mass estimates obtained with the software C-Calcita (Saavedra-Pellitero et al., 2019). Note that the contributions of different coccolith taxa or groups have been indicated (*C.lepto. = Calcidiscus leptoporus;* minor = minor species) and that the data is stacked for each of the approaches. Vertical bars in (b) and (c) represent a 50% error.

875

876 **Table 1: Overview of the samples considered for this study, including the sampling area, number of plankton samples considered**
877 **for this study, expedition, research vessel, water sampling dates, coordinates and data already available from previous publications.**
878

Area	Number of samples considered for this work	Water depth (m)	Expedition	Research Vessel	Plankton sampling period	Coordinates	Previous publications
New Zealand	42	3	XX Italian Expedition	R/V Italica	31.12.2004-06.01.2005	46.81°S to 69.98°S	Coccolithophore assemblages: Malinverno et al. (2015); Dinoflagellates, Coccolithophores, Silicoflagellates, Diatoms, Parmales, Archaeomonads and micro-zooplankton: Malinverno et al. (2016)
Drake Passage	19	5, 10 and 20	Expedition PS97	Polarstern	24.02.2016-05.03.2016	55.44°S to 61.75°S	Coccolithophore assemblages: Saavedra-Pellitero et al. (2019); *Emiliania huxleyi* mass estimates: Saavedra-Pellitero et al. (2019)

879

880

881 **Table 2: Classification scheme of *Emiliania huxleyi* morphotypes observed in the present study (modified from Saavedra-Pellitero**
882 **et al., 2019 and Vollmar et al., 2022)**

***E. huxleyi* morphogroup**	**Morphotype**	**Morphology of the distal shield**	**Morphology of the central area**	**Distal shield length**
A	Type A	Moderately to heavily calcified elements	Grill	< 4µm
	Type A overcalcified	Moderately to heavily calcified elements, broad inner tube	Closed or nearly closed	< 4µm
B	Type B	Lightly calcified elements	Solid plate or laths with irregular outline	≥4 µm
	Type B/C	Lightly calcified elements	Solid plate or laths with irregular outline	< 4µm
	Type C	Lightly calcified elements	Solid plate or laths with irregular outline	< 3.5µm
	Type O	Lightly calcified elements	Opened or lamella	Variable in size

883
884

Table 3: Length, shape factors (Ks) and number of coccoliths per coccosphere used in this work for the New Zealand transect and the Drake Passage transect. (*) Indicates an average of the number of coccoliths per coccosphere. Note that the different Ks used here were mostly based on Young and Ziveri (2000). The shape factor for morphotype O (Ks = 0.015) was introduced by Poulton et al. (2011) in a plankton study along the Patagonian Shelf for a morphotype with a central area described as an "open or thin plate" which the authors called type B/C but that we identified as morphotype O.

Coccolithophore species	Average length ± standard deviation (µm) New Zealand	Average length ± standard deviation (µm) Drake Passage	Source	Ks	Source	Number of coccoliths per coccoshere N. Zealand	Number of coccoliths per coccoshere Drake P.	Source
Calcidiscus leptoporus* spp. *leptoporus	5.7±0.6	5.7±0.6	This work (biometries offshore N. Zealand)	0.08	Young and Ziveri (2000)	15	15	Kleijne (1993)
***Emiliania huxleyi group* A (average value)**	2.95±0.28	3.49±0.33	This work	0.03	This work	15 single layered, 35 double layered	25 (*)	This work (own observations)
***Emiliania huxleyi* A overcalcified**				0.04	Young and Ziveri (2000)			
***Emiliania huxleyi* A (normal)**				0.02	Young and Ziveri (2000)			
***Emiliania huxleyi* group B (average value)**	2.87±0.35	2.98±0.40	This work	0.02	Young and Ziveri (2000)			
***Emiliania huxleyi* B-B/C-C**				0.02	Young and Ziveri (2000)			
***Emiliania huxleyi* O**				0.015	Poulton et al. (2011)			
Gephyrocapsa muellerae	3.9	3.9	Young and Ziveri (2000)	0.05	Young and Ziveri (2000)	15	15	Samtleben & Schroder (1992)
***Syracosphaera* spp.**	2.2	5.5	Young and Ziveri (2000)	0.03	Young and Ziveri (2000)	25	25	Okada & Mclntyre (1977)
Minor taxa			Young and Ziveri (2000)		Young and Ziveri (2000)			Yang & Wei (2003)

Table 4. Summary of MODIS-Aqua products used in this study. (**)The first 8-day period of each year always begins with January 1, the second with January 9, the third with January 17, etc. The final "8-day" composite of each year comprises only five days in non-leap years (27 - 31 December) or six days in leap years (26 - 31 December) (https://oceandata.sci.gsfc.nasa.gov/l3/help/).

				Drake passage transect		New Zealand transect	
Satellite product	**Biophysical variable**	**Extraction method**	**Time period**	**Time span**	**Num. of scenes**	**Time span**	**Num. of scenes**
MODIS-A Level 2	▪ PIC concentration (mol m^{-3}) ▪ Chlorophyll a concentration (mg m^{-3})	mean of 5x5 window centered on measurement location	Daily timestamp	17-02-2016 / 12-03-2016	50	24-12-2004 / 13-01-2005	34
MODIS-A Level 3	PIC concentration (mol m^{-3})	value of pixel enclosing measurement location	8-daily(**) timestamp	10-02-2016 / 12-03-2016	4	26-12-2004 / 08/01/2005	2
MODIS-A Level 3	PIC concentration (mol m^{-3})	value of pixel enclosing measurement location	Monthly timestamp	01-12-2004 / 31/01/2005	2	01-02-2016 / 31/03/2016	2

Table 5. *Emiliania huxleyi* coccolith mass estimates (this study and from other published papers). Note that all the PIC have been converted to pmol per coccolith and the method used has been indicated (Morpho. morphometrics, PLM = polarizing light microscopy, SYRACO = SYstème de Reconnaissance Automatique de COccolithes). The standard deviation has been included whenever it was available.

Geographical area	Sample type	Morphogroup A PIC (pmol)	Morphogroup B PIC (pmol)	*E. huxleyi* PIC (pmol)	Method	Source
Drake Passage	Water	0.0300 (±0.0119)	0.0144 (±0.0062)	0.0166 (±0.0091)	Morpho.	This study
New Zealand	Water	0.0147 (±0.0046)	0.0115 (± 0.0043)	0.0119 (±0.0044)	Morpho.	This study
Drake passage and New Zealand (all samples)	Water			0.013 (±0.0069)	Morpho.	This study
Drake Passage	Water			0.0464 (±0.0253)	PLM (C-Calcita)	Saavedra-Pellitero et al (2019)
Drake Passage	Water			< 0.009	Morpho.	Charalampopoulou et al. (2016)
Off southern Chile	Water			0.013 - 0.015	Morpho.	Charalampopoulou et al. (2016)
Southern Ocean	Laboratory	0.012 to 0.026	0.016 to 0.019		Morpho.	Valença et al. (2024)
Southern Ocean	Laboratory	0.019 to 0.022	0.013 to 0.022		PLM (C-Calcita)	Valença et al. (2024)
Patagonian Shelf (South Atlantic)	Water			0.008 - 0.017 (±0.036)	Morpho.	Balch et al. (2014)
Patagonian Shelf (South Atlantic)	Water	0.019 (±0.007)	0.014 (±0.005)	0.015 (±0.006)	Morpho.	Poulton et al. (2011)
Australian and New Zealand sectors (Southern Ocean)	Sediment trap			0.0264 (±0.0143)	PLM (C-Calcita)	Rigual Hernandez et al. (2020a)
Australian and New Zealand sectors (Southern Ocean)	Sediment trap			0.0099 (±0.006) to 0.0264 (±0.016); mean 0.0181	Morpho.	Rigual Hernandez et al. (2020a)
Indian Southern Ocean (OISO-2004, between 45°S and 59°S)	Water			0.0233 (±0.056)	PLM (SYRACO)	Beaufort et al. (2011)